CELL MODULE AND FUEL CONDITIONER

2ND QUARTERLY REPORT: JANUARY-MARCH, 1980

D.Q. Hoover, Jr.
Westinghouse R&D Center
Westinghouse Electric Corporation
Pittsburgh, PA. 15235

April, 1980

Prepared for
NATIONAL AERONAUTICS AND SPACE ADMINISTRATION
Lewis Research Center
Under Contract DEN 3-161

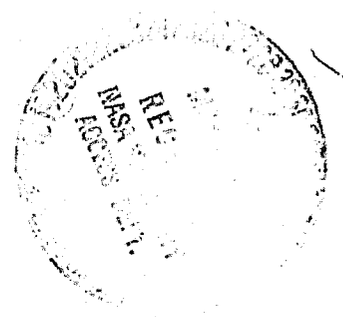

for
U.S. DEPARTMENT OF ENERGY
Energy Technology
Division of Fossil Fuel Utilization
Under Interagency Agreement DE-A1-03-79ET11272

DOE/NASA/0161-79/3
NASA CR-159828

CELL MODULE & FUEL CONDITIONER DEVELOPMENT

2ND QUARTERLY REPORT: JANUARY-MARCH, 1980

D.Q. Hoover, Jr.
Westinghouse R&D Center
Westinghouse Electric Corporation

April, 1980

Prepared for
NATIONAL AERONAUTICS AND SPACE ADMINISTRATION
Lewis Research Center
Under Contract DEN 3-161

for
U.S. DEPARTMENT OF ENERGY
Energy Technology
Division of Fossil Fuel Utilization

TABLE OF CONTENTS

TABLE OF CONTENTS (Continued)

I. INTRODUCTION

This report is for the second Phase of a six Phase program to develop commercially viable on-site integrated energy systems (OS/IES) using phosphoric acid fuel cell (PAFC) modules to convert fuel to electricity. Phase II is a planned two year effort to develop appropriate fuel cell module and fuel conditioner conceptual designs. The fuel cell module development effort comprises three coordinated tasks:

Task 1: Design of Large Cell Stacks

Task 2: Stack Fabrication

Task 3: Stack Testing

The "Fuel Conditioner Subsystem Development" task is the fourth technical task of this effort. Provision for "Management, Reporting and Documentation" is included as a fifth task.

The work accomplished during this reporting period is described at the subtask level in the following section.

II. TECHNICAL PROGRESS

TASK 1: DESIGN OF LARGE CELL STACKS

1.2 Stack Design

Thermal Management

Due to differences in temperatures and material of various components, changes in stack temperature result in differential thermal expansions which, in turn, alter the extent of stack compression.

A preliminary theoretical analysis of the thermal expansion behavior of the major components of an 80-cell stack (i.e., bipolar plates, aluminum compression plates, Teflon insulators, compression pads, bars and rods) was made for the three cases listed in Table I. The thermal behavior of the electrodes, matrix and shims was not included in the analysis due to uncertainties about their material properties (such as coefficients of thermal expansion and the nature of the relationship between deformation and applied pressure). These components constitute less than 8% of the overall height of the stack. The results of this analysis (Table I) indicate an increase in cell compression for typical operating conditions (Case C).

TABLE I

Case	Predicted Change in Dimensions	Net Effect
A. Perfectly insulated i.e. all components are at 178°C (350°F)	Expansion of the tie rods exceeds that of the stack by .017 in.	Compression is decreased
B. Tie rods at 56°C (exposed to room temperature), stack (including tie bars) at 178°C.	Expansion of the stack exceeds that of the tie rods by .012 in.	Compression is increased.
C. Typical operating conditions. Tie bar and tie rod temperatures measured (70-90°C and 60°C respectively).	Expansion of the stack exceeds that of the tie rods by .010 in.	Compression is moderately increased, i.e., the increase is less than that of Case B.

Bipolar and Bipolar/Cooling Plate Design

Modifications to be incorporated in the bipolar and bipolar/cooling plates for the second 23 cell stack of the Mark I design (DIGAS) are:

1. An acid reservoir channel will be machined into the seal area of the anode side of the bipolar plate. Acid fill holes are located at each end of this channel.

2. There are to be thirty (30) cooling channels of an innovative design in each bipolar/cooling plate.

   a. Each channel is to be 0.22 in deep.

   b. All channels will have same dimensions but the spacings between channels will vary.

   c. The channels will be machined with smoother transitions and a 45° chamfer will be machined into the channel entrances to reduce flow resistances.

   d. A new method of joining the bipolar/cooling plate halves will be selected to reduce IR resistance. A method which may be used is discussed in section 2.1.

Other modifications from previous stack procedures are as follows.

1. The acid reservoir channel will be at the air flow exit (hot) side of the plate where acid loss is highest.

2. Acid will be added to the matrix prior to assembly (wet assembly).

3. Additional acid is to be added to the stack via the acid fill holes. Scheme I* for limiting the head of acid in each cell to very low values is to be incorporated in this new stack build.

*Described in a patent disclosure which will be separately submitted to the NASA program manager.

1.3 Full Scale Module Designs

The full scale module enclosure (manifolds, seals, compression plates, etc.) design advanced to the point that a design review is appropriate. A letter outlining the design's functions, its description, the problems to which it speaks and a procedure for assembling the enclosure and the stack is being issued, preparatory to a design review scheduled for April. This letter includes copies of the assembly and detail drawings of the enclosure. The estimated cost of the enclosure (including materials, labor, equipment depreciation, ROI, etc.) is $25 per kW.

A clamping device was conceived which allows the processing and testing of five cell subassemblies. The current plan is to fill the matrix with phosphoric acid prior to or during assembly. This will permit visual inspection of the acid filled matrix before covering it with the next electrode layer. Vendors of the equipment needed to produce bipolar plates and electrodes nave been contacted for cost data.

The bench mark cost data for the repeating components was completed. The results will be presented at a NASA review meeting scheduled for April 8th. The platinum content in the electrodes is by far the largest cost factor. Without platinum the cost per kilowatt is approximately $100 as calculated by NASA's interim price guideline costing model. This includes depreciation for equipment, buildings and a profit on the producer's assets.

Several concepts for automated assembly of the repeating stack components have been completed. Based on these assembly concepts, four workers (two per shift/day) should be capable of assembling the repeating components for 16,700 stacks/year.

TASK 2: STACK FABRICATION

2.1 Methods and Approach to 8 kW Stack Fabrication

Cooling Plate Assembly

Preliminary evaluation of the contact resistance attained with several alternative surface treatments of the contact areas between cooling half plates was made. The objective is to eliminate the graphite paper and thus simplify cooling plate assembly, reduce pressure drop in the direction of flow and enhance the temperature uniformity of the cells. The resistances for several candidate treatments are shown for several compression levels in Table II. The effects of curing at room and elevated temperatures and of several compression cycles for two cooling plates assembled with the graphite suspension are shown in Table III. The resistances shown were measured across a 12.5 cm x 38.1 cm assembly of 2 compression plates, 2 current collectors, 2 sheets of graphite paper, and the two bipolar/cooling plate halves. Hence, they are only indicators of the effect of surface treatment on the contact resistance between cooling plate halves.

Since the graphite suspension eliminates the problems associated with backing paper, is simple to apply during stack fabrication, requires only an overnight cure at room temperature, and the material that remains after curing is essentially graphite (and should be compatible with other stack components and able to withstand stack operating conditions) it is a prime candidate for replacing backing paper in cooling plate fabrication.

The improved handling procedure shown in Table II includes removal of mold release compound and storage in a closed atmosphere.

Border Seals

The border seals of the DIGAS cooling plates are an important factor in preventing reactant or cooling gas crossover. Since the graphite suspension is not an adhesive, it may not serve as a sealant. Experiments were conducted using epoxy and heat-sintered FEP as border sealing compounds. The preliminary results shown in Table III indicate

TABLE II

EFFECT OF SURFACE TREATMENT METHODS
ON COOLING PLATE CONTACT RESISTANCE

	RESISTANCE, mΩ		
Surface Treatment \ Compression, psi	30	45	60
Set 1			
Improved Handling	7.9	5.75	5.35
220 grit sandpaper	6.55	5.40	4.85
with backing paper	4.0	3.55	3.35
graphite suspension	6.35†	5.05†	3.30‡
Set 2			
Improved Handling	6.40	4.90	4.40
220 grit sandpaper	4.00	3.30	3.10
with backing paper	3.55	3.20	3.00
graphite suspension	4.10†	3.40†	2.65‡
Set 3			
Improved Handling	6.85	4.85	4.65
solvent (MEK)	5.75	4.60	4.30
with backing paper	3.65	3.35	3.20
Set 4			
Improved Handling	6.5	5.55	5.20
with backing paper	4.0	3.55	3.45
graphite suspension	6.2†	4.95†	4.50†

* Based on untreated sample
† Taken initially; no time allowed for curing
‡ Taken after 12 hours of curing

TABLE III

EFFECT OF CURING AND PRESSURE CYCLES
ON CONTACT RESISTANCE OF COOLING
PLATE ASSEMBLED WITH GRAPHITE SUSPENSION

	RESISTANCE, mΩ		
Surface Treatment \ Compression, psi	30	45	60
Set 1			
Graphite suspension (RT) (initial)	6.35	5.05	4.35
14 hrs at 220°F (104°C)	----	----	3.10
Decompress (RT)	3.40	3.30	3.10
Recompress (RT)	4.25	3.70	3.40
Decompress (RT)	3.90	3.60	3.40
Recompress (RT)	4.50	3.70	3.35
Decompress (RT)	3.80	3.40	3.35
(Samples held together after disassembly)			
Set 4			
Graphite suspension (RT) (initial)	6.2	4.95	4.50
14 hrs RT	----	----	3.30
Heating to 310°F (154°C)	----	----	3.35
Cooling to RT	----	----	3.35
Decompress	3.60	3.42	3.35
(Samples came apart during disassembly)			

that, with a epoxy and graphite suspension applied to the first and last rib and to one rib in the middle, a permanent seal is established without increasing contact resistance significantly and that the seal can withstand variations in temperature and compression.

Another method of sealing the DIGAS plates involves the use of an O-ring type seal along the 12 in. edges of the plates. Grooves were machined into the borders of a half plate to accomodate a 12 in. long cylindrical Viton strip cut from an O-ring. Viton strips, with a diameter approximately 30% greater than the groove depth, were laid in the grooves and the other cooling half plate placed on top. When the stack was compressed, the O-ring strips formed an acid resistant, gas-tight seal along each edge. This type of assembly was incorporated into a ten-cell stack (built under an Army program at Energy Research Corporation) which has been in operation for a few months. The O-ring type seal is performing successfully without any additional resistance (15 mV ohmic loss at 100 mA/cm^2) through a cooling plate.

Electrolyte Filling

Electrolyte filling of the matrices (initial filling and replenishment of acid) is a vital aspect of stack fabrication and operation. The following experiments are being conducted to develop improved filling techniques and methods for quantifying the completion of filling.*

A 3 cell 12.7 cm x 38.1 cm stack was built and wicked using innovative techniques which are described in patent disclosures submitted separately to the NASA Program Manager. The resistance of the stack and the flow rates of acid into and out of the stack were monitored. The wicking of the stack was completed in 20 hours (as indicated by no further decrease in stack resistance and a flow of acid out of the stack equal to the flow in) at an acid flow of 4.5 cc/hr. Table IV lists estimates of the amount of acid required to fill the stack based on calculated porosities of the components under compression. These compare favorably with the value of 51 cc measured during the experiment.

*Appendix A is a description of an experiment performed to verify Scheme I.

TABLE IV

THEORETICAL ESTIMATION
OF ACID INVENTORIES IN THE STACK

Component	VOLUME OF ACID, cc Under Compression	
	Minimum	Maximum
Matrix	40.2	40.6
Anode	0.6	4.5
Cathode	1.2	8.7
Reservoir	1.7	1.7
Total	43.7	55.5

To obtain data on the effects of vertical wicking and verify the use of stack resistance as a measure of acid filling the following experiment was performed. A single 12.7 cm x 38.1 cm cell was assembled with an oversized (12.7 cm x 40.6 cm) Kynol matrix. The stack was assembled with the same nominal compression (60 psi) as the 3-cell stack described above and supported with the 40.6 cm dimension vertical. The excess matrix length (2.5 cm) was exposed at the bottom and submerged half way in a container of ~100% acid in the dry room and its temperature was maintained at 104°C. The electrolyte filling was monitored by observing the change in color (from light gold to dark brown) of the matrix edges. The decrease in stack resistance with time was also recorded. As indicated in Figure 1, the stack visually appeared to be filled after 7 days but stack resistance continued to decrease until the 8th day. Post-test analysis of the matrix showed complete wicking. Therefore, eight days should be adequate to vertically wick a 30.5 cm x 43.1 cm stack under compression. This has been corroborated with 5 cell stacks (successfully wicked in 9 to 12 days) built under the DOE Technology Program.

Materials Compressibility

Experiments were initiated to characterize the deformation of the electrodes and matrix when compressed between the bipolar plates. In these initial tests, electrodes, matrix, and graphite backing paper were compressed between smooth blocks and compressed under 100 psi and 200 psi. At 200 psi, typical of the MK-1 design, the materials were reduced in thickness by about 25% (Table V). As shown in Table V, the reduction in thickness at 100 psi, which is typical of the MK-2 design with the same force applied to the stack, the reduction in thickness is about 80% of that at 200 psi. A single matrix layer was compressed to 1000 psi and its thickness was reduced about 44.4% (0.0083 in). Calculations indicate that the porosity of the matrix would be reduced from a value of 70% (in the uncompressed condition) to 58% at 200 psi and 47% at 1000 psi.

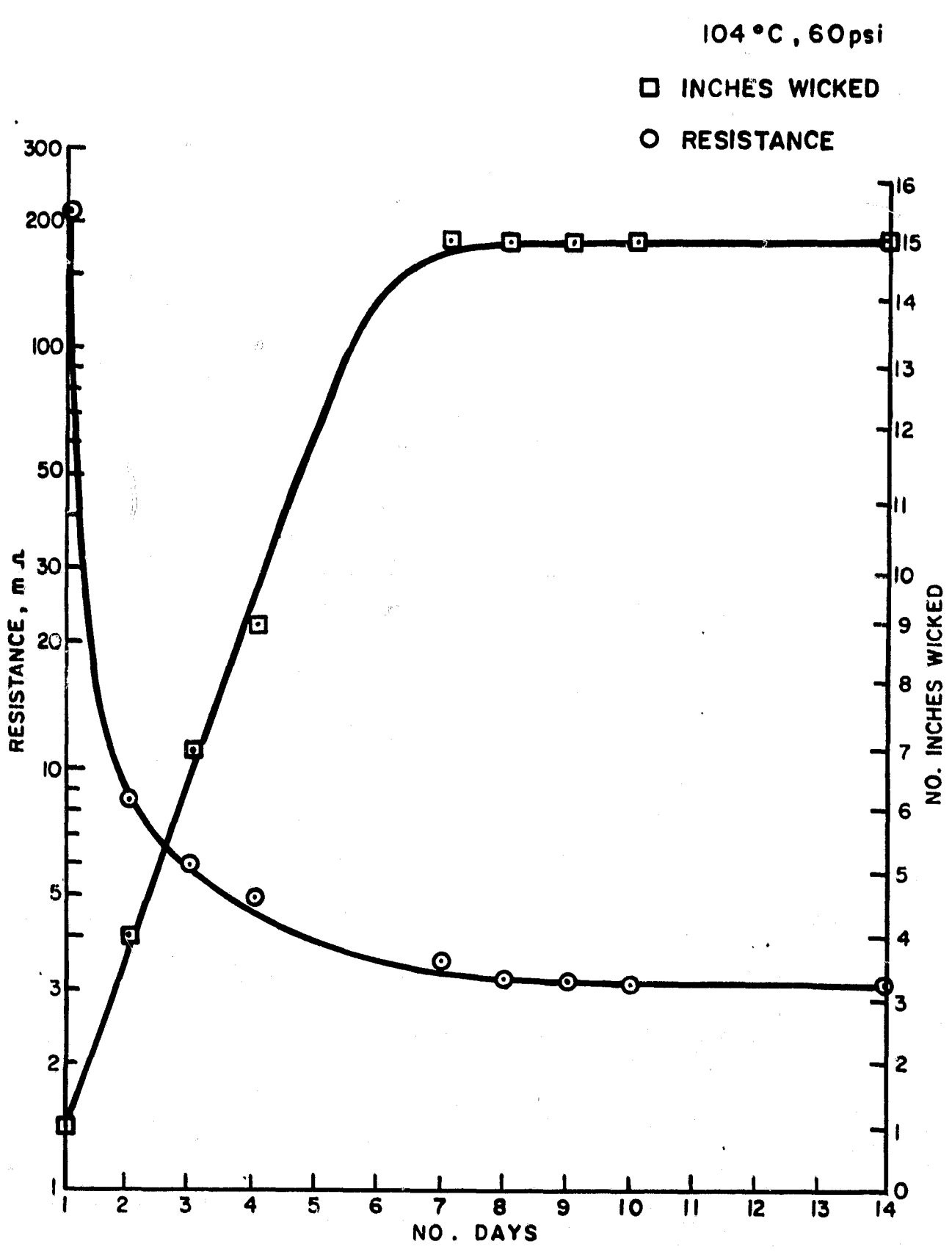

FIGURE 1 STACK A WICKING DATA

D1061

TABLE V

COMPRESSION TESTS OF FUEL CELL COMPONENTS
(SMOOTH BLOCKS)

Component	Original Thickness (in)	Reduction in Thickness	
		200 psi in (%)	100 psi in (%)
Composite (A+C+M)	0.057	0.0114 (20)	0.0093 (16.3)
Matrix (M)	0.0187	0.005 (26.7)	0.0036 (19.3)
Anode (A)	0.0167	0.0037 (22.2)	0.0031 (18.6)
Cathode (C)	0.0207	0.0038 (18.4)	0.0028 (13.5)
Graphite Paper	0.014	0.0034 (24.3)	0.0027 (19.3)

2.2 Simulated Stack Fabrication

Assembly of Stack 557 (the first MK-2 simulated stack) was completed on January 9, 1980. After 25 days of wicking, stack internal resistance, OCV measurements, and leak tests indicated the matrices were filled. The stack was put on test and the results are discussed under Subtask 3.2.

TASK 3: STACK TESTING

3.2 Simulated Stack Testing

Testing of Stack 557 (the first five-cell stack of the MK-2 design) was initiated when internal resistance and open circuit voltage measurements indicated that the matrices were filled with acid. Initially, cell performance averaged 0.53 V/cell at 100 mA/cm^2 and 0.90 V/cell OCV at 177°C. After a few hours operation, performance deteriorated to 0.50 V/cell and 0.80 V/cell OCV at the same conditions. Polarization data taken during this period showed an oxygen gain of 98 mV/cell at 100 mA/cm^2, which indicated the existence of a diffusion restriction at the cathode. The falling OCV and increasing IR (from 3.7 to 5.2 mΩ) indicated the possibility of a crossleak which was corroborated by a leak test.

Post-test analysis of Stack 557 components indicated that certain areas of the matrix had not been fully wicked. These areas were in a pattern that indicated a direct relationship to the rib pattern of the MK-2 bipolar plates. Procedures to eliminate this problem will be implemented in the second MK-2 simulated stack.

3.3 Short Stack Testing

Stack 556 (a 23-cell stack of the MK-1 design) was installed and tested in the Westinghouse loop and performance was stable at the same level obtained at ERC.

Polarization curves shown in Figure 2 were obtained at five temperature levels between 124 and 182°C. This data was analyzed by the techniques developed in Phase I to obtain resistance and catalyst utilization as a function of temperature. Table VI shows the resistance and catalyst utilization factor at the five stack temperatures.

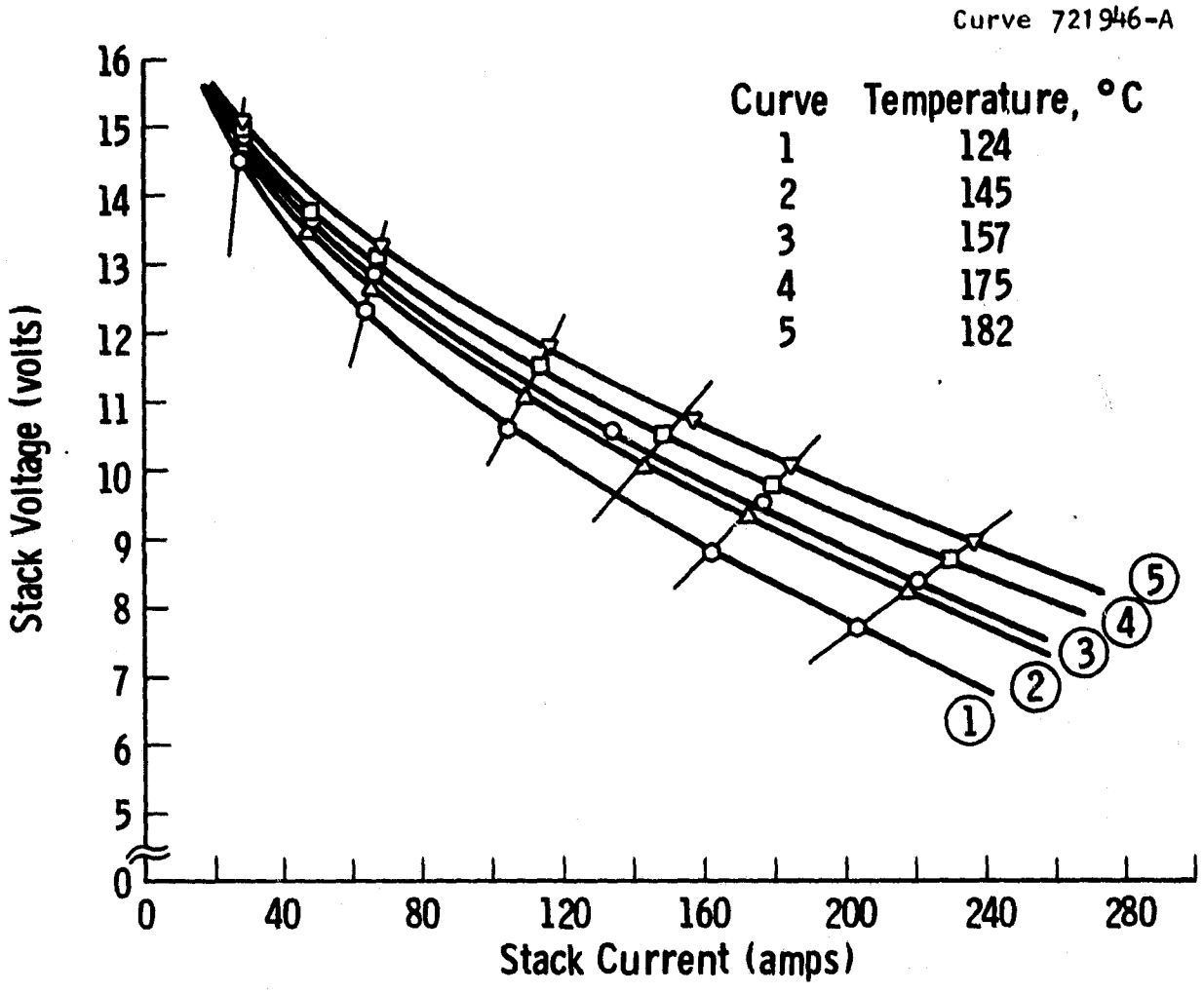

Fig. 2—Polarization curves for stack 556 (31 × 43 cm)

TABLE VI

SPECIFIC RESISTANCE AND CATALYST UTILIZATION

FOR STACK 556

Temperature °C	Specific Resistance Ohm-cm^2	Catalyst Utilization Factor
124	1.426	.0137
145	1.219	.0179
157	1.190	.0234
175	1.064	.0245
182	0.971	.0274

The temperature distribution along the air flow direction at the center of the stack was measured on six separate occasions at a current of 110A. Five tests were made at an air flow with a calculated air rise of 58°C. These tests showed a bipolar plate temperature difference (from outlet to inlet edges) of 48°C. One test at an air flow with a calculated air rise of 83°C showed a plate temperature difference of 52°C.

In order to further investigate the temperature distribution, the stack was instrumented with six additional movable thermocouples which were used to obtain complete temperature distributions for cell 12 and cell 17. The distribution on cell 12 is shown in Figure 3 for unheated fuel and in Figure 4 for heated fuel conditions. A local hot spot was found near the hydrogen inlet at the air exit edge of the cell. The distribution on plate 17 shown in Figure 5 was then obtained to verify that a similar distribution occurred on other cells in the stack. The fuel inlet half of Figure 5 was obtained one day and the fuel exit half of the distribution was completed later under slightly different conditions.

Two transient type tests were conducted to determine the thermal conductivity and the specific heat of the stack. With the stack isothermal at no current, a load was suddenly applied. Temperatures throughout the central region of the cell increased at 10°F/minute during the first 1.5 minutes. For a cell thickness of .18" (.457 cm) and a cell voltage of 0.510 volts, the calculated ρc (density x specific heat) product is 0.423 cal/cm^3/°K. In the second test the stack was allowed to equilibrate from an initial linear temperature distribution without air flow. The temperature changes during a time interval were used to calculate the thermal diffusivity (α) of the stack in the air flow direction. Then $k = \rho c \alpha$ was used to calculate thermal conductivity (k). The average value obtained for k was 0.141 W/cm-°C. Previous analyses have been made using k = 0.341 W/cm-°C. This lower value of thermal conductivity accounts for part of the higher than expected temperature difference from air outlet to inlet sides of the cell.

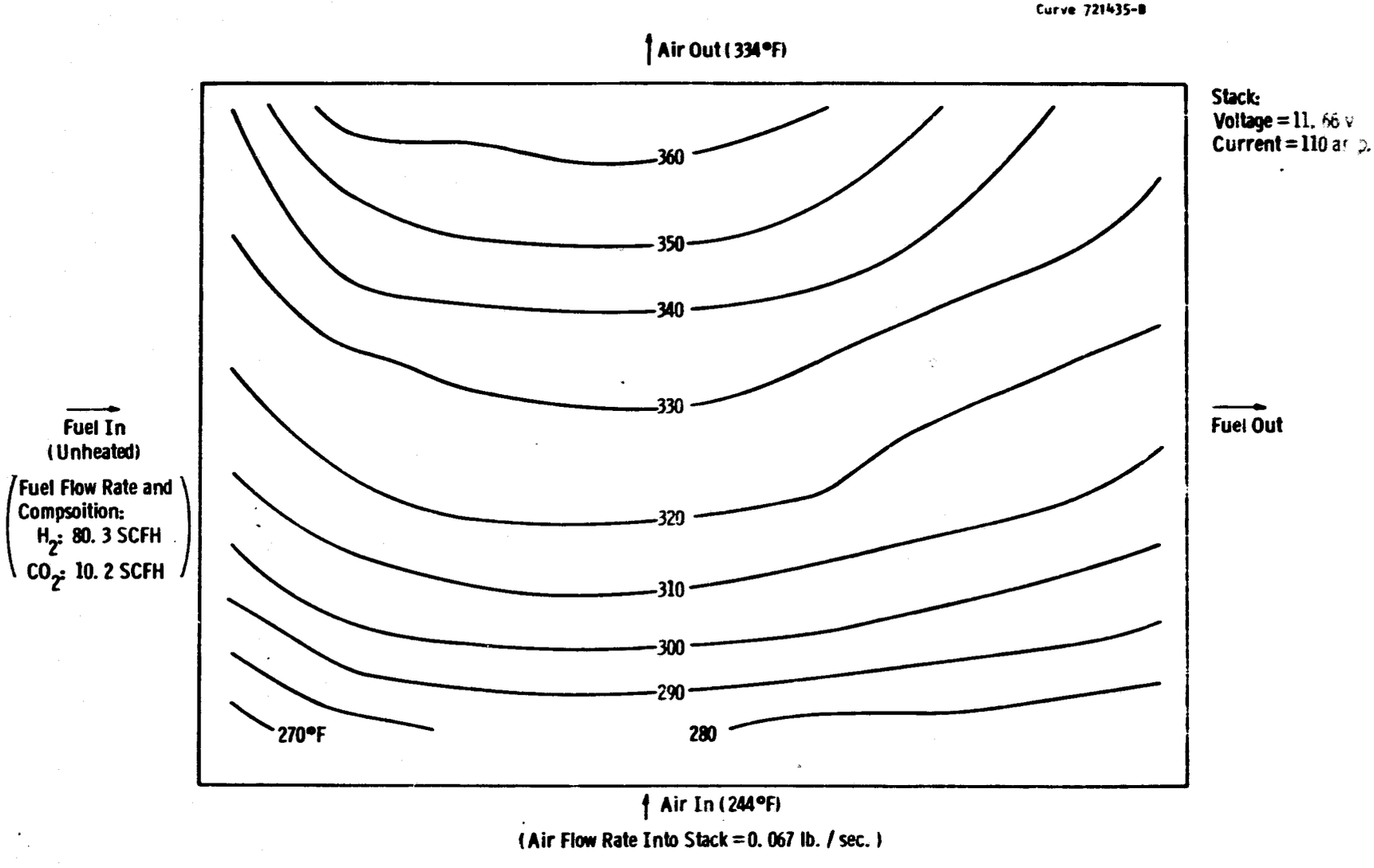

Fig. 3 — Isothermal contours measured on bipolar plate # 12 in stack 556. (No fuel heating)

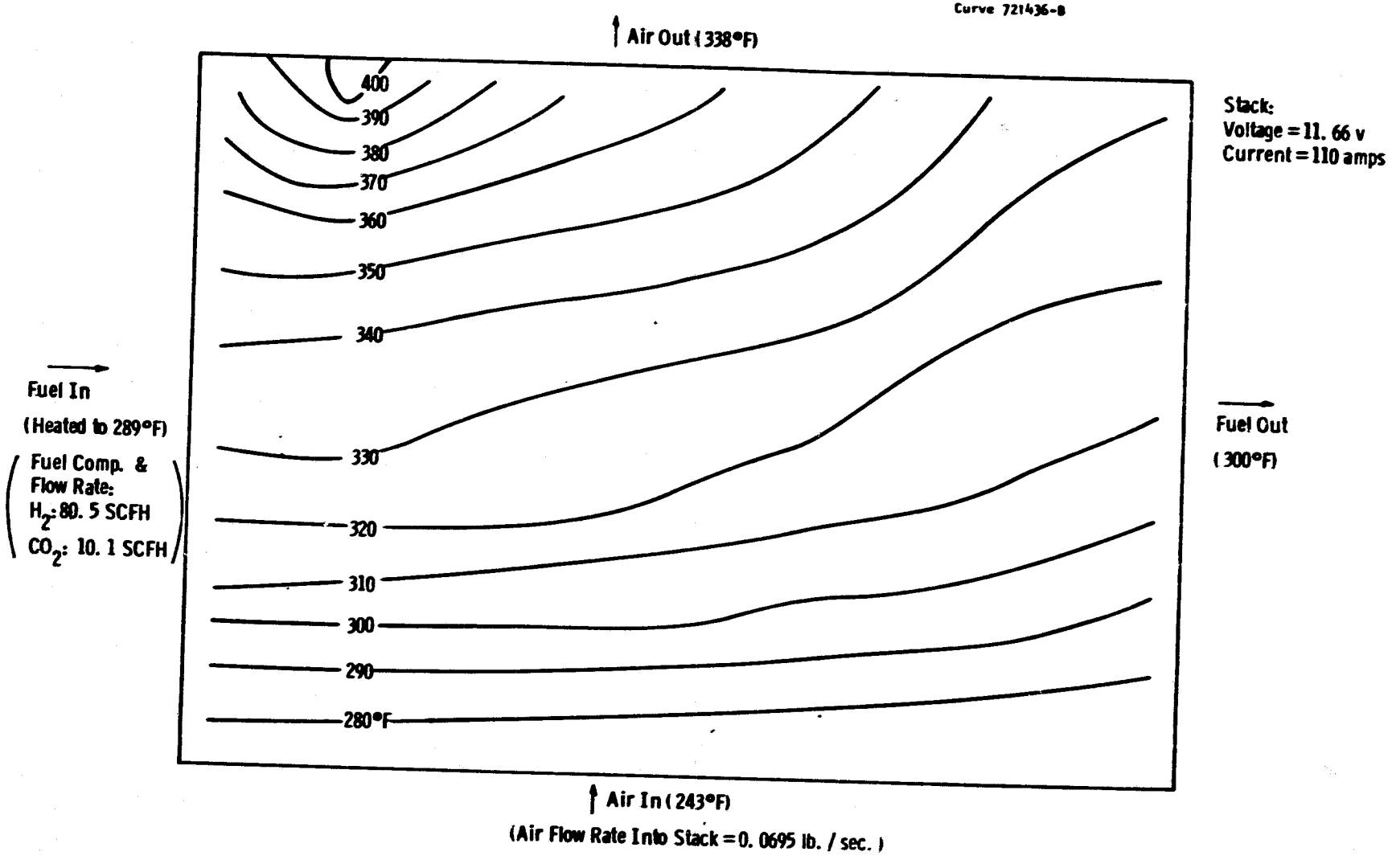

Fig. 4 — Isothermal contours measured on bipolar plate # 12 in stack 556 (with fuel heating).

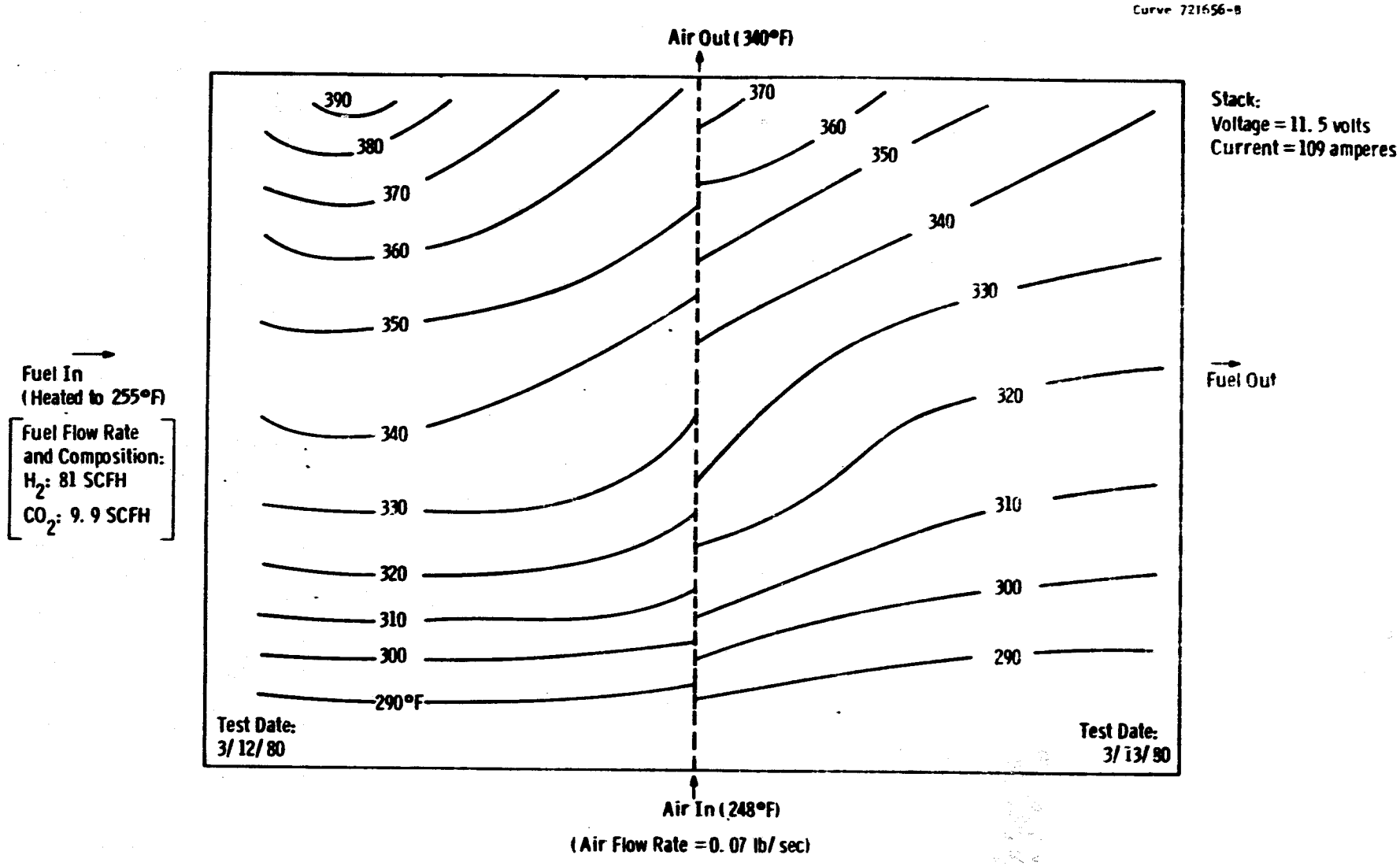

Fig. 5 — Isothermal contours measured on bipolar plate #17 in stack 556.

During transient tests it was observed that the hot spot persisted even at zero current when hydrogen was supplied to the cell, indicating a local crossover. Records of prior tests were reviewed and it was found that the hot spot was present in previous isothermal tests when high fuel flow rates were present at low current, indicating a crossover.

The restrictive exit fuel line was replaced with a larger line and a test was made to observe whether heating occurred at zero current when fuel was supplied to the stack. The temperature distributions obtained in this test along the center of cell 12 are shown in Figure 6. The top portion of Figure 6 shows the air flow, current, and fuel flow sequence used. The stack was initially at steady state with a current of 110 A, 2 stoich fuel flow, and air flow corresponding to a 56°C rise. Air flow, fuel flow, and current were reduced to zero for 15 minutes. Then air flow was resumed for 15 minutes without fuel or current. The temperature profile at this time is shown as curve 1 of Figure 6. The air inlet temperature was maintained at 150° ± 2°C throughout the remainder of the sequence at constant air flow. At time 1, cold fuel flow was turned on to one half the initial steady state flow rate for 15 minutes. Curve 2 shows the temperatures at the end of period 2. Note that temperatures increased significantly above air inlet throughout the cell. Fuel flow was then increased to the initial rate for period 3 and the temperatures increased to values shown by curve 3. Fuel flow was reduced in period 4 and the essentially steady state conditions reached are shown by curve 4. Fuel was turned off again in period 5. Curve 5 shows that temperatures were approaching the air inlet temperature at the end of the period. These results show significant heating throughout the cell and severe localized heating near the air exit side of the cell. Essentially identical results were obtained for cell 17 indicating that conditions were similar throughout the stack. It is believed that the crossover leaks indicated by this test were the cause of low voltage performance and poor temperature uniformity obtained.

Curve 721947-A

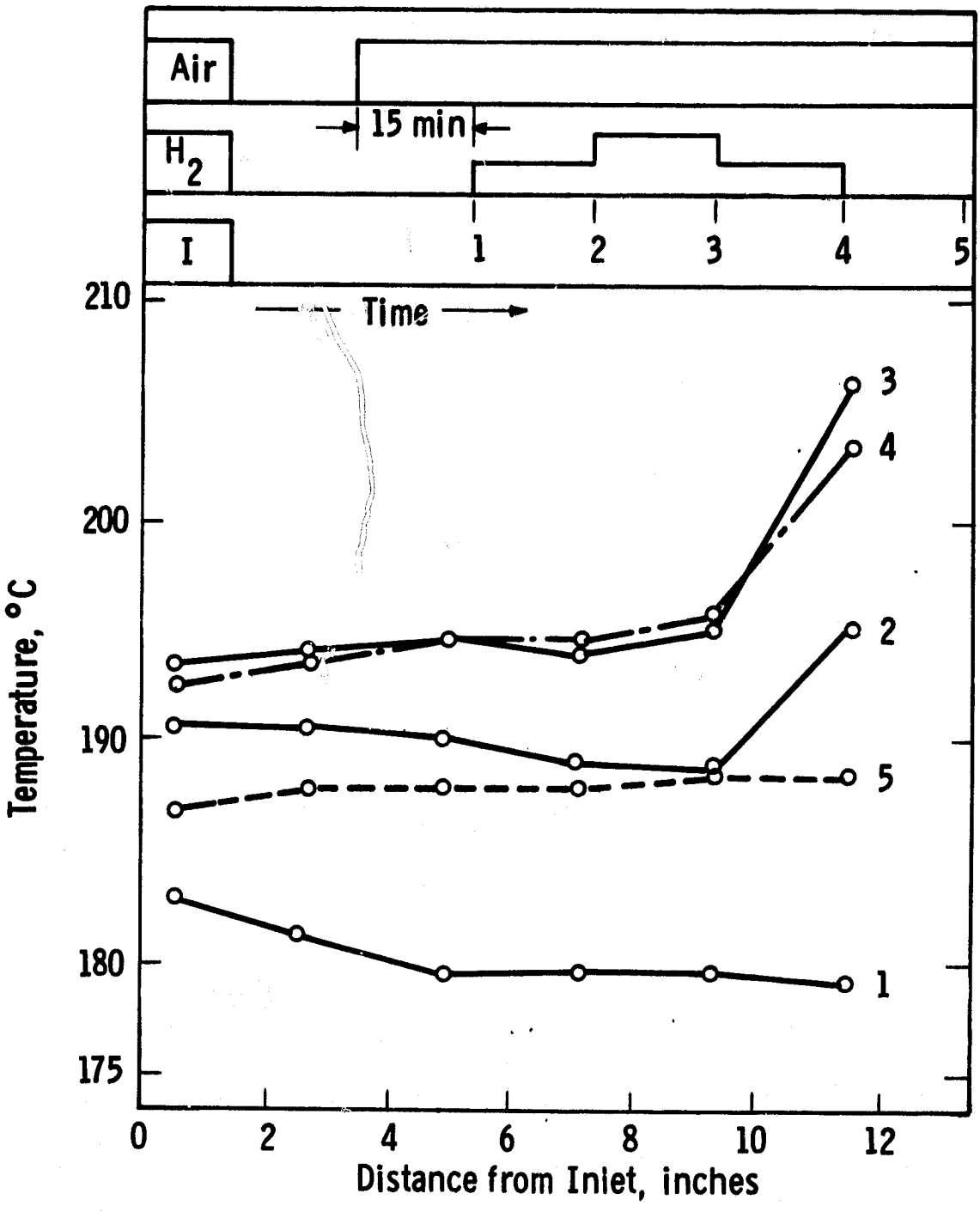

Fig. 6—Temperature distributions for zero current reaction test

In order to measure the flow characteristics of the process channels of Stack 556, the cooling channel inlets were plugged. The pressure drop vs flow curves at 29°C and 121°C are shown in Figure 7. The measured pressure drops at .025 lb/sec are 68 percent higher than predicted by the detailed analytical model. These results indicate that actual channel dimensions must be 12.3 percent smaller than those used in the pressure drop calculation. This difference could be due to .013 cm (.005 inch) sag of the electrodes into the process channels.

3.4 Test Stand Design and Construction

The design of a test facility for short stacks (23 cell, 30 cm x 41 cm) was submitted to and approved by the NASA program manager. The salient features of this test facility are:

Automatic Control

- of fuel composition and flow rates
- of stack exit air temperature

Safety Features

- stack overheating prevention
- ΔP monitor across cell and stack to prevent over-pressurizing the cell
- H_2 level monitor in air stream and in room
- guards against electric power failure
- automatic shutdown operation

Operation

- automatic data scanning and recording
- round-the-clock unsupervised operation

Flow Ranges (SCFM)

Gas Streams	Nom.	Max.	Min.
Hydrogen	1.5	2	0.4
Carbon Dioxide	0.35	0.5	0.1
Carbon Monoxide	-	0.07	-
Air Makeup	5	90	3
Loop Air	60	130	15

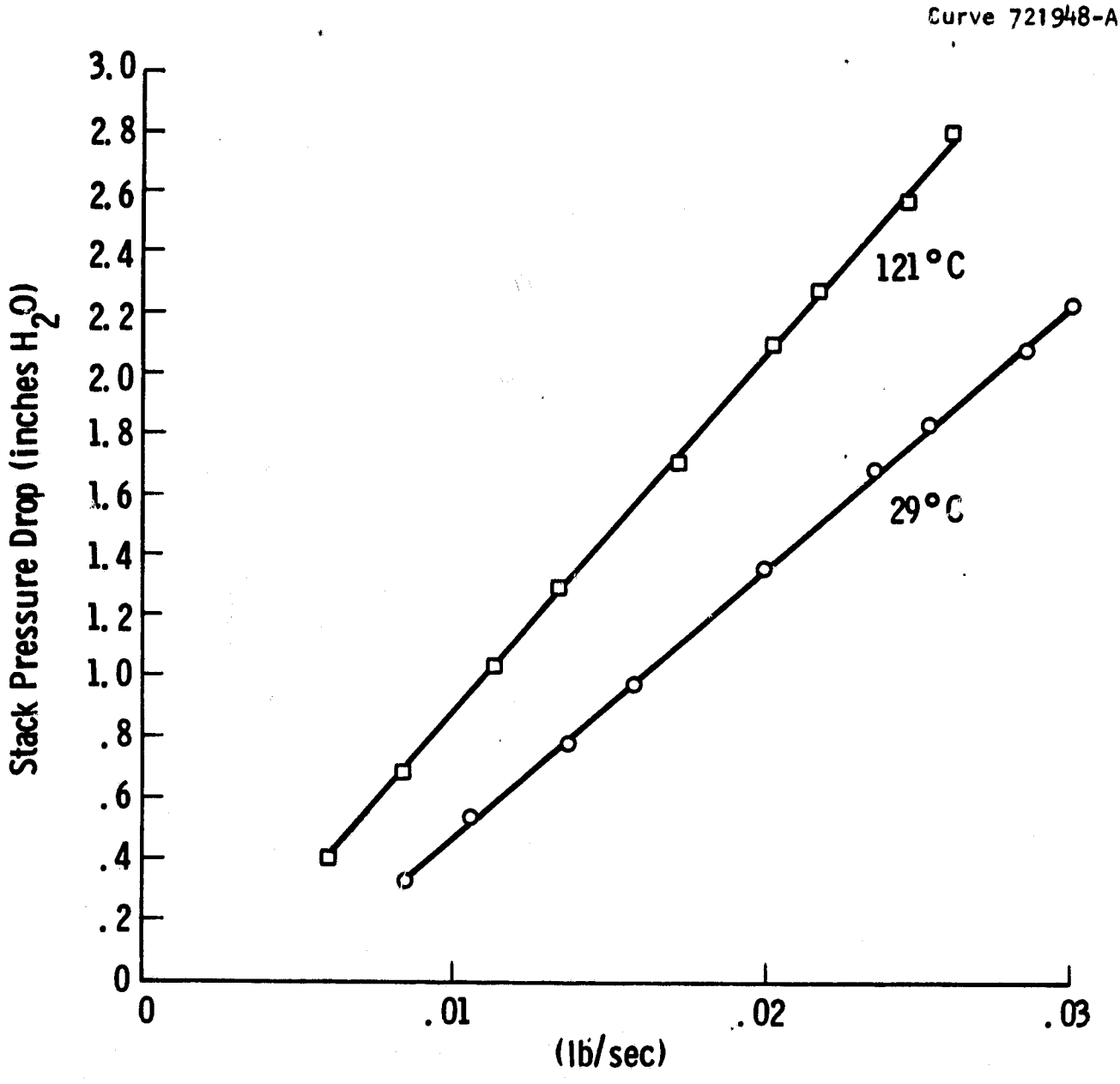

Fig. 7—Air flow vs pressure drop (process channels only of stack #556)

Operating Parameters

- external load
- cell and air temperatures
- reactant compositions
- reactant utilization

Measurements

- cell voltage
- current output
- air flow rates
- fuel gas composition and flow rates
- temperatures - air, fuel, cell and stack
- pressure in all streams (also monitor ΔP across cell and stack)
- water content in air and fuel exit streams
- oxygen concentration in air stream

All of the above measured parameters and operational parameters will be logged in a data acquisition system.

Fuel and Air Control Loops

Figure 8 is a schematic of the fuel cell testing facility.

Fuel (H_2, CO_2 and CO) will be supplied from individual cylinders. The control valves (V3 through V5) will blend the gas streams in preset proportions. This fuel blend will be passed through the anode humidifier (AH) and the fuel preheater which will control the inlet temperature of the fuel mixture to the stack.

Filtered room air will be drawn in by the blower and supplied to the stack. The total flow rate into the stack will be measured by a turbine flowmeter (F1) and will be controlled manually by valve V1. The air preheater will be used mainly for startup. The exit gas from the stack cathode will be partially vented. For control of the outlet temperature of the recycled flow, the recycled stream will be divided into two streams: through a heat exchanger and through a bypass.

FIG. 8 MK-I STACK
2 kW TEST STATION

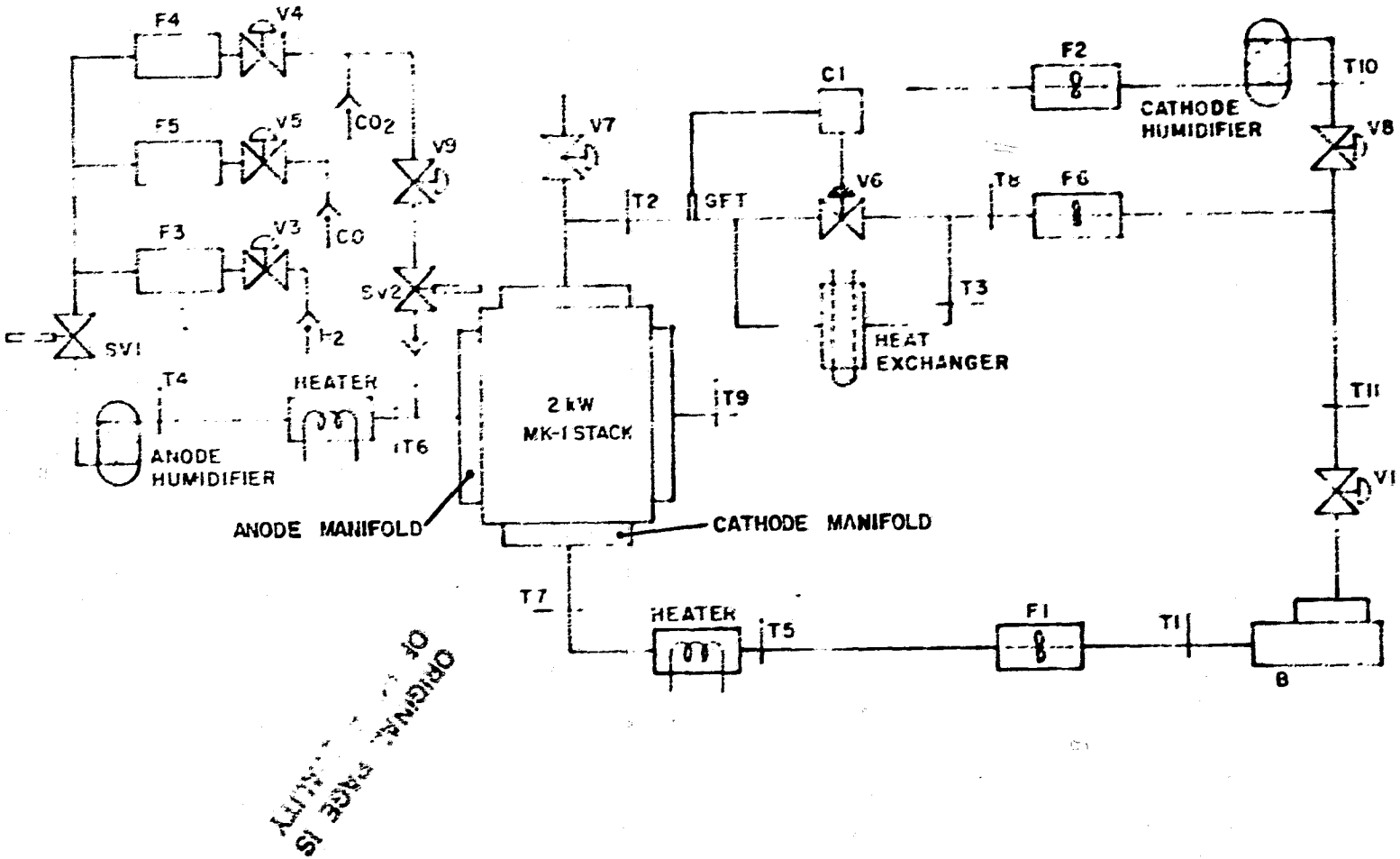

The desired flow ratio (i.e., through the exchanger vs through the bypass) will be controlled by valve V6. The mixing ratio of the recycled stream with the makeup air will be controlled by another valve, V8, and their flow rates will be individually measured by flowmeters F2 and F6. The air flow loop is designed for as much as 70 stoich flow for a 2 kW stack.

Since too high a stack operating temperature, i.e., 400°F (204°C) or higher, results in stack component damage and too low an operating temperature adversely affects performance, the control of the stack temperature is important. Controller C1 will adjust the flow through the heat exchanger to maintain the preset stack outlet air temperature, T2. This will be accomplished for any given recirculation ratio and total air flow rate (set by V1 and V8). When the exit air temperature changes, e.g., rises above the set point, GFT* in the exit air manifold will send a signal to controller C1. C1 will then close V6 to pass more air through the heat exchanger to lower the recycle stream temperature. This will lower the inlet air temperature until the air exit temperature is back to the desired set point. With this type of control, the total air and recirculation flow rates can be maintained independent of stack temperature.

Alarm Monitoring

A data acquisition system (DAS) will scan all temperature and voltage data input channels to protect the stack. The DAS will provide HI and LO or HI-HI or LO-LO alarms for each input channel. Each alarm will be used for a warning signal and will be assigned a relay output to initiate an ON/OFF control action as needed.

*GFT is a gas filled thermometer which can be connected directly to the pneumatic controller C1. To produce the same action using the signal from a thermocouple (T2) would require the use of a temperature transmitter and a current to pressure transducer. Thus the use of GFT is more economical in this case.
However the thermocouple, T2, is used for data logging and ON/OFF control.

Temperature Protection

If the stack temperature increases to Alarm Level, say 375°F (191°C), then stack shutdown procedures will be activated. The load will be taken off the stack and, at the same time, the fuel feed line and preheater will be shut off and solenoid valve SV2 will be activated to purge the system with CO_2. A timer can be set to limit the purge time to conserve CO_2. In the case of timer malfunction, the system will still be purged but the CO_2 cylinder will be drained. Once the alarm is activated, the system can only be reset manually.

ΔP Monitor Across Cell and Stack

To prevent damage to the cell matrices, the air side pressure should remain close to the hydrogen side pressure. Pressures in the fuel and air exits will be continuously monitored and connected to the alarm and shutdown system. A liquid sealed relief valve (Figure 9) is also attached to the air line. Submerged depth, H, will be determined based on the safe exit air pressure with respect to the fuel exit pressure and the specific gravity of the liquid used. Because of the relatively high air temperature, a nonvolatile liquid will be selected for this application.

H_2 Level Detector

H_2 concentration in the air exit stream and in the room will be continuously monitored. Should a H_2 leak develop and exceed either of the preset values, it will trigger the alarm which will immediately begin shutdown procedures as described previously and the room exhaust fan will also be activated. The system will require manual reset.

Electric Power Failure

Electric power failure will result in turning off the fan and the H_2O pump. It will also close the shutdown relay and result in releasing the external load, bringing all valves to a predetermined, fail safe position. Also the fuel valve will be closed and CO_2 purging will be activated. The system will then have to be manually reset for operation.

TASK 4: FUEL CONDITIONER DEVELOPMENT

4.1 Fuel and Water Definitions

4.1.1 Fuel Definition

The OS/IES fuel conditioning system could be designed to utilize any of the various gases that enter an urban apartment house through the natural gas supply pipe. The effort this quarter has been concentrated on narrowing the spectrum of gas compositions to those gases that will permit a simple, cost effective fuel conditioner to serve the largest part of the potential OS/IES market. Data collected during the previous quarter were analyzed and discussed with NASA Lewis and Jet Propulsion Laboratory personnel, and the following conclusions were made:

1. Propane/air peak shaving gas would not be processed by the OS/IES system. This relieves the fuel conditioner design from the necessity to deal with high oxygen content gases (in the 3% to 15% range) and the potential for catalyst sintering provided by those gases. Also propylene (C_3H_6), introduced as a normal content of commercial propane, with its strong ability to deposit carbon in the reformer, would not need to be hydrogenated to propane to avoid reformer catalyst deactivation.

2. The exclusion of propane/air peak shaving gas from the design will not prevent the addition of an oxygen removal reactor with heat exchangers and a propylene hydrogenation reactor with increased hydrogen recycle when and if needed. These future additions would be contained in an add on package for which connections and space will be provided in the present system design.

3. The range of natural gas compositions considered, with averages for each constituent, will be:

Composition, Vol %	Range	Average
CH_4	72.4 to 95.15	89.4
C_2H_6	2.5 to 11.32	5.1
C_3^+	0.71 to 5.07	1.9
N_2	0.3 to 17.1	2.9
CO_2	0 to 1.98	0.7
He	0 to 0.34	-
	TOTAL	100.0

These compositions represent over 150 individual natural gas sources in the U.S., and represent nearly all of the actual natural gas compositions that the OS/IES system will be required to process.

4. Oxygen content is tentatively set at 0.3% maximum. This limit may be extended to 3% maximum after discussion with catalyst manufacturers regarding the tolerance of their sulfur removal catalysts to oxygen. The higher limit would permit processing natural gas that has been diluted with air, a practice of some east coast utilities during peak demand periods.

5. Sulfur compounds in the gas, including odorant materials required by law such as mercaptans and hydrothiophenes, will be set at 20 ppm V maximum. This will require removal via a hydrodesulfurization (HDS) reactor and a zinc oxide bed. Carbon adsorption of sulfur compounds cannot compete with HDS due to the physical size of the adsorption system and the high cost and complexity of sulfur recovery from regenerable carbon adsorbers.

6. SNG synthesized from coal will be an acceptable feedstock. Generally such gas is rich in hydrogen and has lower C_3^+ contents than normal natural gas which makes it quite suitable as an OS/IES feedstock.

7. Coke oven gas and gas synthesized from oil will be excluded from OS/IES designs. These gases provide complications in design due to olefins such as C_2H_4 and traces of NH_3. In general, an olefin level of 0.2 vol % will be used for the OS/IES system. Since the use of oil derived gas and of coke oven gas in natural gas supply systems is small and is decreasing, such an olefin limit should not significantly restrict the OS/IES market.

8. The pressure levels established for gas lines entering residential units by the various state utility commissions will be the basis for OS/IES design. These pressures are 2 inches water gauge minimum and 20 inches water gauge maximum. They are detailed for individual states in the American Gas Association standards for home appliance manufacture. Standards are presently being prepared by the American Gas Association for residential fuel cell use.

9. Water content is generally specified as one pound per million standard cubic feet of natural gas. To prevent freezing in the gas meter at the OS/IES site, the gas dew point must be below minimum ambient temperatures. This very low level of water is negligible for OS/IES design purposes.

Discussions will continue with catalyst manufacturers regarding the capabilities of their hydrodesulfurization, reforming, and shift catalysts to tolerate impurities. However, the definition of natural gas for this program will in general be as discussed above.

4.1.2 Water Definition

Work continued during this quarter on identifying water compositions which will be available to the fuel conditioner subsystem of the phosphoric acid OS/IES fuel cell. This water will be used to produce steam for reforming of pipeline gas to a fuel suitable for the fuel cell.

The design flow schematic for the water recovery system shown in the Oct-Dec 1979 Quarterly Report continued to be used. This schematic depicts water being recovered by condensation from the spent fuel and exhuast air waste streams. It is based on the design philosophy requirement that all process steam to be used in the reforming operation be produced from water recovered in the system.

Based on results of their experimental work, ERC has suggested that the P_4O_{10} levels in the gas streams to the exhaust air and spent fuel condensers might be no higher than 0.5 ppm (vol). Calculations of water compositions have been revised to reflect this lower level.

Table VII shows the estimated gas and phosphoric acid content of the individual and combined water streams, on the basis of 0.5 ppm (vol) P_4O_{10} in the respective gas streams. Also shown are the hourly flow rates of water and P_4O_{10} along with the corresponding temperatures of each stream.

The combined composition will be used as a preliminary basis for the water conditioner design choices in Task 4.4. A new system definition based on natural gas compositions and reformer performance appropriate for those gas compositions is being prepared in Task 4.2 for this work. Also, in Task 4.4, the option of potable water use is being explored relative to water conditioner cost and to system regeneration and waste disposal. A revised set of water compositions will be provided after the new system definition is available.

4.2 Operational Requirements Definition

Work has begun on revising the state point diagram. The natural gas composition provided by Task 4.1.1 above will be the basis for revision. Also, reformer performance at nominal full load (120 kW) and quarter load (40 kW) will be provided. This work will be completed in May of 1980 and will provide revised input to the other fuel conditioner development tasks.

TABLE VII

ESTIMATED COMPOSITIONS OF RECOVERED WATER STREAMS

Values in ppm (by wt)

	Combined	Exhaust Air	Exhaust Spent Fuel
PO_4 (as $CaCO_3$)	67.5 (106.6)	77.6 (122.6)	33.5 (52.3)
CO_2	76.7	--	328.0
CO	0.1	--	0.5
H_2	0.1	--	0.5
CH_4	<0.05	--	<0.2
O_2	6.6	3.6	--
N_2	11.3	12.1	--
Water Temp °F	110.9	104.5	132.0
Water GPH (PPH)	18.1 (150.9)	13.9 (115.6)	4.2 (35.3)
P_4O_{10}, PPH	7.6×10^{-3}	6.7×10^{-3}	0.9×10^{-3}

4.3 Technical Data Base

Upon completing the construction of the test facility, a series of tests were initiated to check out the performance of this unit. The equipment operated satisfactorily for the test conditions shown in Tables VIII and IX. Following these tests, the reactor was filled with 1.6×10^{-3} ft^3 (4.5×10^{-5} m^3) of 1/8 inch (3.18×10^{-3} m) inert alumina spheres. The pressure drop for a broad range of flow rates was determined, as shown in Figure 10. From this a bed of material was chosen for the experimental phase of this work as shown in Figure 11. The total gas space velocity of the chosen configuration will be approximately 4,000 hr^{-1} and a very small pressure drop will result. This value will vary to a small extent depending on the flow rates required to keep the conversion below 20%. The configuration shown in Figure 11 was tested with Haldor Topsoe RKNR catalyst (described in the First Quarterly Report) and the conversion was below 20% at a space velocity (based on total volume of the bed) of 4,000 hr^{-1} and a temperature of 1000°F (538°C). A test with only the alumina pellets indicated no conversion.

The shakedown testing of this reactor was completed by February 29, 1980. The catalyst bed and inlet gas flows used in the shakedown test are given in Table VIII. "Space velocities" based on gas volume and weight flow rates and on total volume and weight of catalyst rings are given in Table IX. The "theoretical hydrogen out" is the amount of hydrogen which would be produced by complete conversion of the incoming methane according to the equation:

$$CH_4 + 2H_2O \longrightarrow CO_2 + 4H_2$$

TABLE VIII

FUEL CONDITIONER

SPACE VELOCITIES

(Shakedown)

Haldor Topsoe RKNR

Ni Catalyst-wgt.=0.5g=(1.10 x 10^{-3} lbs.)

Catalyst Bed Volume (w/support)=1.07cc.(.001071)=(3.77 X 10^{-5} $ft.^3$)

Gas-In Ratios: .1 CH_4
.4 H_2O
.48 He
.02 H_2

Total Vol. Gas in=.625 lpm CH_4 + 2.51 lpm H_2O+3.01 lpm He+.125 lpm H_2
= 6.25 lpm.

S.V. for entire support and catalyst = 4166 hr^{-1}

Total Wgt. Gas in=.0112 g H_2/min
+.4464 g CH_4/min
+2.0089 g H_2O/min
+.5357 g He/min
= 3.0022 g/min

TABLE IX

FUEL CONDITIONER

SPACE VELOCITIES

	Total Gas In	CH_4 in	Theoretical H_2 out
$\frac{\text{Vol. gas}}{\text{Vol. Bed}}$	350,000 hr^{-1}	35,000 hr^{-1}	140,000 hr^{-1}
$\frac{\text{Wt. gas}}{\text{Wt. Catalyst}}$	360 hr^{-1}	53.6 hr^{-1}	26.8 hr^{-1}
$\frac{\text{Wt. gas}}{\text{Vol. Bed}}$	10,500 $\frac{lb}{hr\ ft^3}$	1,560 $\frac{lb}{hr\ ft^3}$	781 $\frac{lb}{hr\ ft^3}$

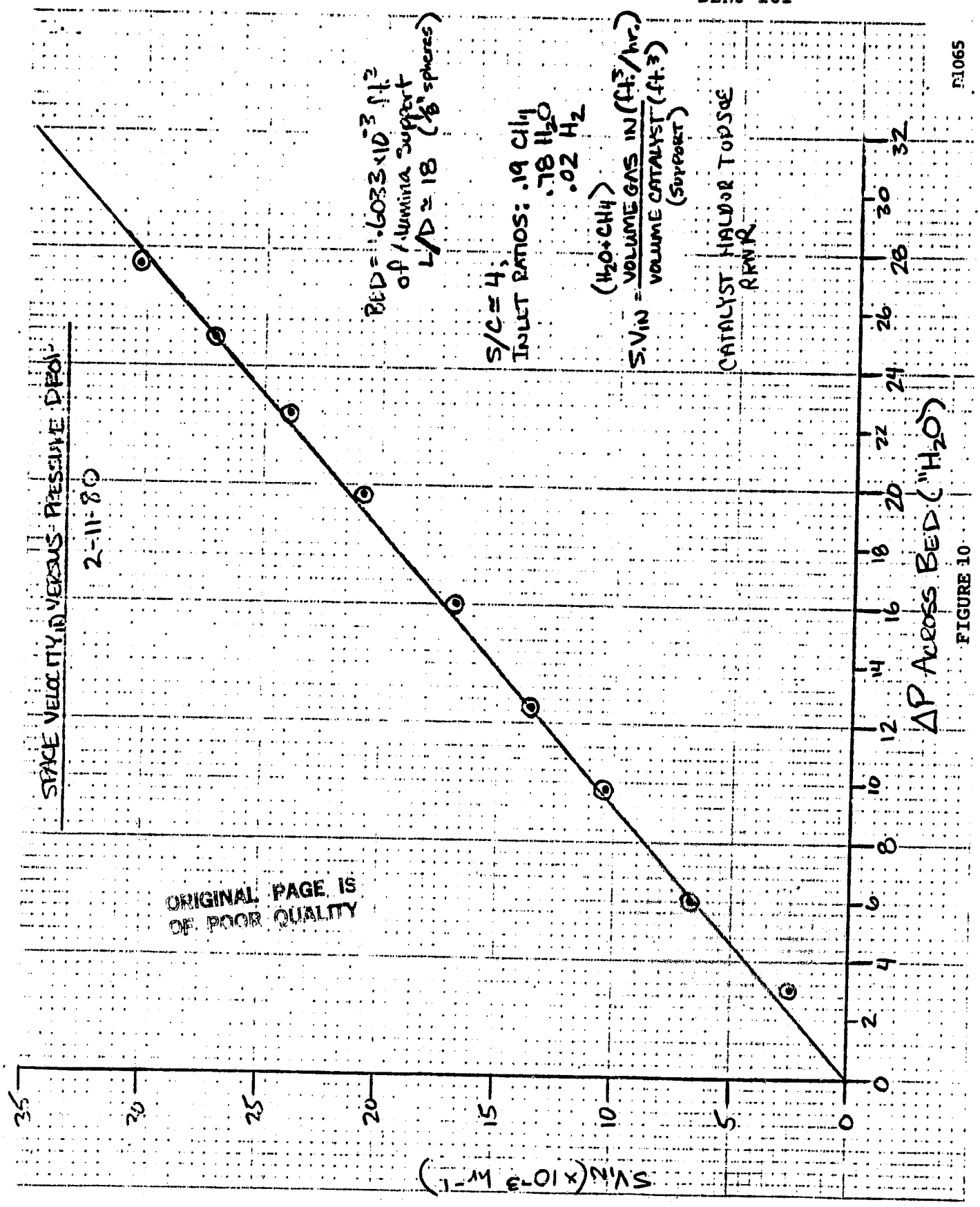

FIGURE 10

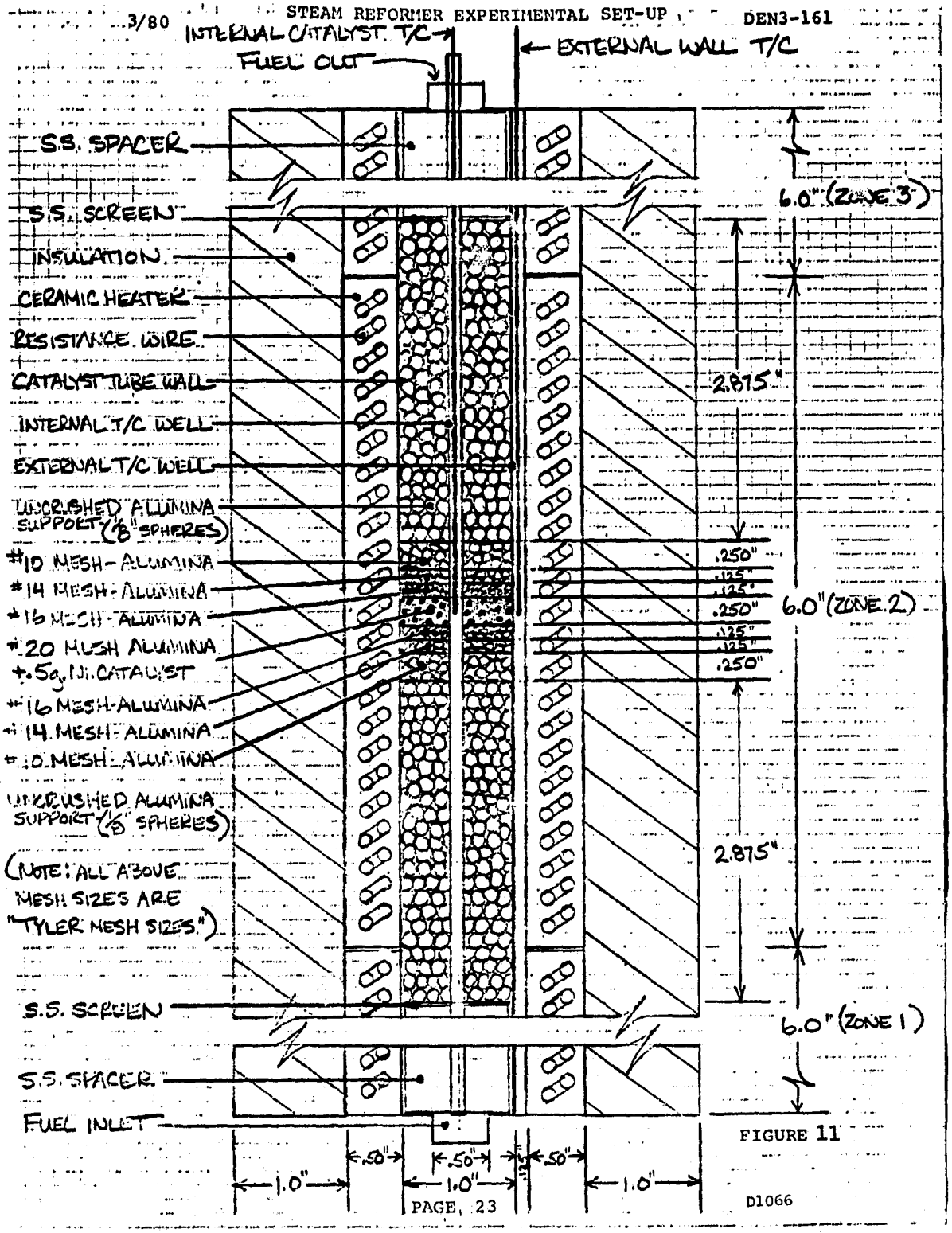
...3/80
STEAM REFORMER EXPERIMENTAL SET-UP
DEN3-161
INTERNAL CATALYST T/C
FUEL OUT
EXTERNAL WALL T/C
S.S. SPACER
S.S. SCREEN
INSULATION
CERAMIC HEATER
RESISTANCE WIRE
CATALYST TUBE WALL
INTERNAL T/C WELL
EXTERNAL T/C WELL
UNCRUSHED ALUMINA SUPPORT (⅛" SPHERES)
#10 MESH - ALUMINA
#14 MESH - ALUMINA
#16 MESH - ALUMINA
#20 MESH ALUMINA
+.5g Ni. CATALYST
#16 MESH-ALUMINA
#14 MESH-ALUMINA
#10 MESH-ALUMINA
UNCRUSHED ALUMINA SUPPORT (⅛" SPHERES)
(NOTE: ALL ABOVE MESH SIZES ARE "TYLER MESH SIZES.")
S.S. SCREEN
S.S. SPACER
FUEL INLET
6.0" (ZONE 3)
2.875"
.250"
.125"
.125"
6.0" (ZONE 2)
.250"
.125"
.125"
.250"
2.875"
6.0" (ZONE 1)
.50"
.50"
.50"
1.0"
1.0"
1.0"
PAGE, 23
D1066

FIGURE 11

4.4 Ancillary Subsystem Data Base

4.4.1 Burner Development

Test Rig

Reformer burner development has proceeded in three distinct areas: 1) the design, 2) the hardware procurement, and 3) the detailed drafting of how the procurement parts as well as those fabricated in the shop will fit together. The design tasks included the size of the burner and its port facilities, the development and detailing of the burner geometry and establishing the necessary components for a small and portable facility. Once the individual components were specified in size, the hardware procurement was started. The burner is sized for supplying a 60 kW fuel cell so that two units can be used in parallel for a 120 kilowatt system. Each burner will use 113 pounds per hour of air and 73 pounds per hour of anode effluent gas at full load. The burner passage itself will be rectangular in cross section, approximately 6" wide by 2" high and 18" long. A header for the air supply, which will disperse the total airflow through a series of small holes to insure uniform air delivery, will be located in the upstream section. This will be followed by a section with screens to insure a uniform velocity distribution across the entire section. Eight inches downstream a flame holder will be located to anchor the flame. The gas is supplied from a cylindrical plenum through a series of small holes into the gas distribution flame holder chamber. The dimensions of the flame holder are 1" wide extending completely across the 6" width. The upstream end of the flame holder is a half cylinder while the downstream end is blunt (Figure 12 shows a magnified section of the flame holder). In this blunt end, the gas and the air are expected to mix and burn rapidly and completely at low emission levels. The burner section is followed by a heat transfer section where the gas can be cooled by water cooled walls. The gas heat transfer section will be completely instrumented so that the enthalpy change of the gas can be measured as well as the heat absorption by the water cooling. This

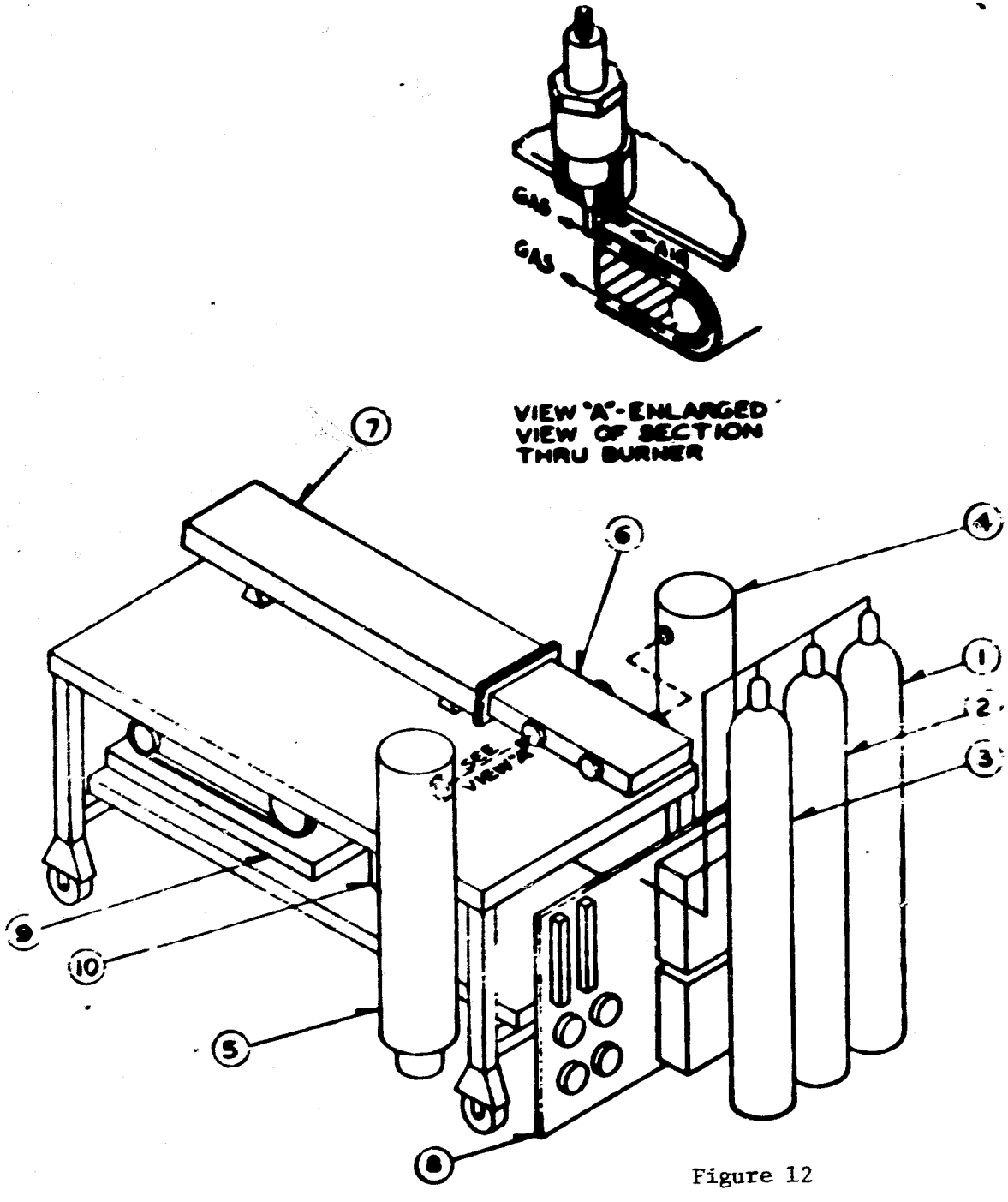

Figure 12

LEGEND

1 CH_4 GAS CYLINDER
2 N_2 GAS CYLINDER
3 FUEL MIX CYLINDER
4 AIR HEATER
5 GAS HEATER
6 BURNER
7 COOLING CHAMBER
8 CONTROL PANEL
9 AIR BLOWER
10 GAS SATURATOR

FUEL CELL BURNER TEST RIG

section is so designed that fins and other extended surfaces as well as packed beds can be installed to measure heat transfer from these enhancement devices. Such devices may be crucial to the proper operation of the reformer. The system including the burner is shown on Figure 12 and consists of a blower supplying the air to an air heater which then will be delivered to the burner. The gas introduced in the flameholder can be one of three different compositions, supplied by individual cylinders. The first is methane, which will be used as a startup fuel. The second is the actual fuel mixture to be supplied by Matheson, Airco or similar gas supplier in the required amount and composition shown on Table X. The third, nitrogen, will be used to purge the system. Flows will be measured by flowraters. Controls are also provided to permit precise temperature control on both the air and gas in the electric heater. The gas will be saturated at about 100°F in a thermostatically controlled water bath in which the saturators are immersed.

Once the individual components for the system described in Figure 12 were specified, hardware procurement for these items was started. The status of the hardware procurement is shown in Table XI. All major components have been received. Drafting has been completed for the assembly, control panels, and other necessary items required by the apparatus shown in Figure 12.

TABLE X

FUEL GAS COMPOSITION

	Mole Percent
CH_4	3.5
CO	2.9
H_2O	7.3
CO_2	47.0
H_2	39.3

TABLE XI

HARDWARE STATUS

Item	Item Order Date	Promised Delivery	Received	
9 kW air heater	1/11/80	4/3/80	4/11/80	
7.5 kW gas heater	1/11/80	4/3/80	4/11/80	
Controls for above heaters	1/11/80	4/3/80	4/11/80	
Air blower w/bed plate	10/30/79	2/14/80	2/25/80	
Motor for blower	10/30/79		11/8/79	
Portable bench	2/20/80	3/7/80	3/17/80	
2 rotameters	2/15/80	3/14/80	3/31/80	(1 received)
Gas saturation bottles	2/20/80		3/4/80	
Immersion heater	2/20/80		3/6/80	
Battery jar	2/20/80		3/4/80	
Thermometer	2/20/80		3/4/80	
2 pressure gauges	3/24/80	4/14/80		
2 thermometers w/stems	3/24/80	4/14/80		

Heat Transfer Model Verification

The following is a description of the continuing effort to verify our heat transfer model by comparing the calculated results with tube wall and gas temperatures data provided by the NASA Project Manager. To match the data, heat transfer coefficients that are higher than any known correlation must be used in the calculation.

Briefly reviewing, the analysis of the DOE 40 kW reformer heat transfer characteristics which was reported in the previous quarterly report resulted in the heat balance for a differential element, dx, of the reformer tube and gives the following differential equation;

$$h \pi D\, dx\, (TG-TW) = \dot{w}\, C_p\, d(TG) \qquad (1)$$

where

- h = heat transfer coefficient at the wall
- C_p = specific heat
- D = diameter of tube where heat transfer occurs
- $\dot{w}$ = mass flow rate of gas
- x = axial length of tube in flow direction
- dx = differential length
- TG = combustion products temperature
- TW = wall temperature

this can be transformed to:

$$K \frac{dY}{d\eta} + Y = TW \qquad (2)$$

where

- $Y = TG$
- $\eta = x/L$
- $K = \dot{w}\, C_p / h \pi D L$
- L = length of heat transfer surface in x direction.

If the wall temperature TW can be represented by an equation of

$$TW = a + b\eta + c\eta^2 \qquad (3)$$

the solution for the combustion gas temperature is

$$TG = TW - bK + 2cK^2 - 2cK\eta + (TGO - a + bK - 2cK^2) \times (\exp(-\eta/K)) \quad (4)$$

The heat transfer in the reformer tube between the gas and the reformer tube wall must be the heat absorbed by the reforming gases. The pertinent values for the reformer are shown in Figure 13. The required energy for a reformer tube supplying 10 kilowatts of fuel cell output would be 18,110 Btu since the specific heat load shown in Figure 13 is 1,811 Btu per kilowatt.

In reference 1, three tube wall temperatures are given. The top of the tube had a temperature of 1630°F (1160°K), the mid point 1400°F (1033°K), and the bottom 800°F (700°K). Since the combustion gas leaves the reformer at 740°F (667°K) and the reforming reactants enter at 400°F (478°K), the end temperature should lie between those limits and the "bottom of the tube" temperature of 800°F (700°K) must be upstream of the end point. Since, in our minds, some uncertainty exists about the geometric definitions of the "top of", "the midpoint" and "the bottom" of the tube, two wall temperature distributions were considered as shown in Figure 14. Temperature distribution 1 (TW1 in Figures 15, 16, and 17) essentially places these temperatures at the start, midpoint and near end of the convective section. Temperature distribution 2 (TW2 in Figure 16) spreads this distribution over the actual length including the radiant section upstream of the convective section as shown in Figure 13. Introducing these values into the gas temperature equation and adjusting heat transfer coefficient to provide a 667°K combustion gas exit temperature from the reformer results in the curves of gas temperatures shown in Figures 15, 16, and 17. For

(1) Letter from United Technology Corporation to NASA dated August 18, 1978.

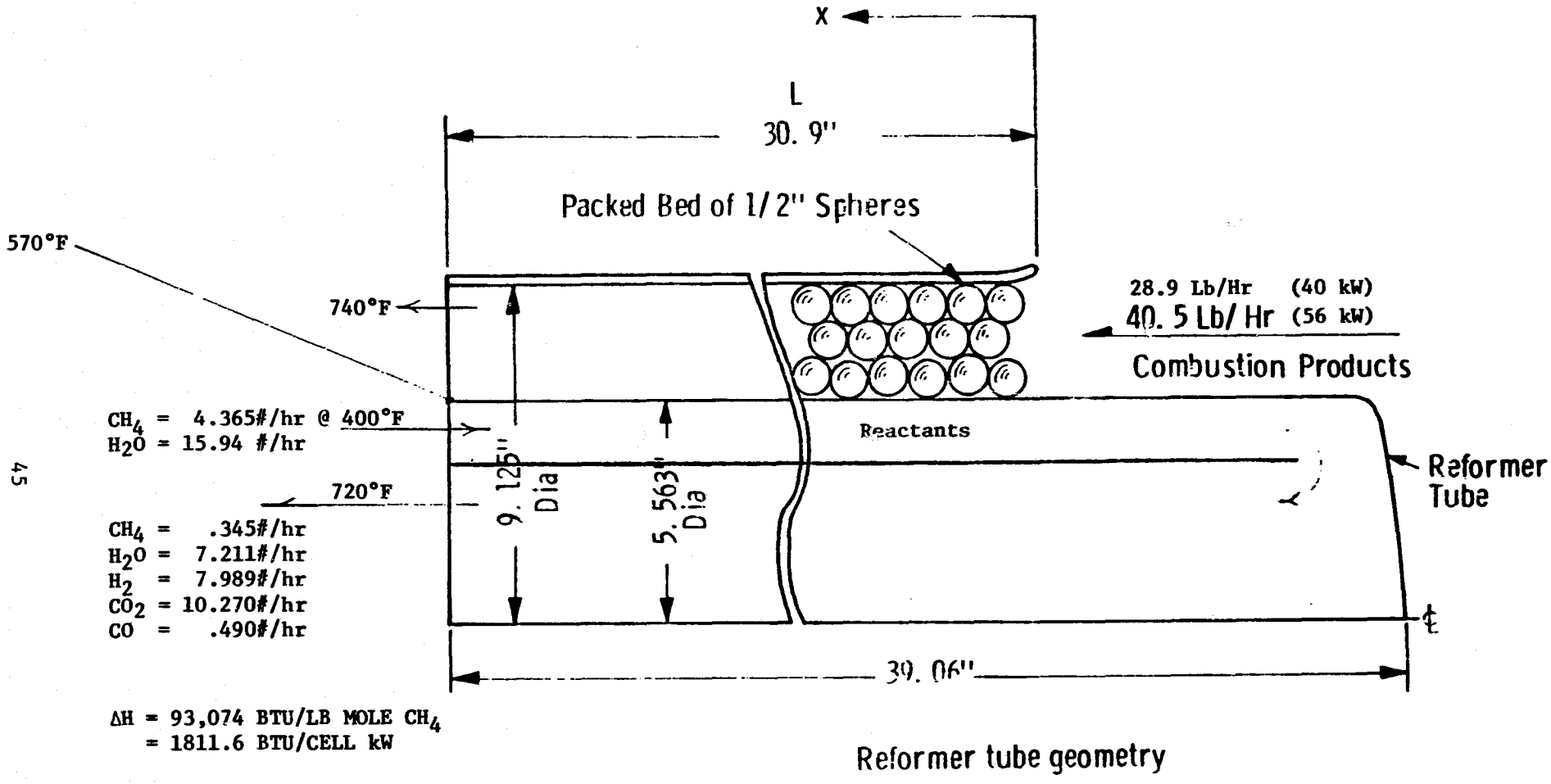
X
L
30. 9"
Packed Bed of 1/2" Spheres
570°F
740°F
28.9 Lb/Hr (40 kW)
40. 5 Lb/Hr (56 kW)
Combustion Products
CH4 = 4.365#/hr @ 400°F
H2O = 15.94 #/hr
Reactants
Reformer Tube
720°F
9. 125" Dia
5. 563" Dia
CH4 = .345#/hr
H2O = 7.211#/hr
H2 = 7.989#/hr
CO2 = 10.270#/hr
CO = .490#/hr
39. 06"
ΔH = 93,074 BTU/LB MOLE CH4
= 1811.6 BTU/CELL kW
Reformer tube geometry

FIGURE 13

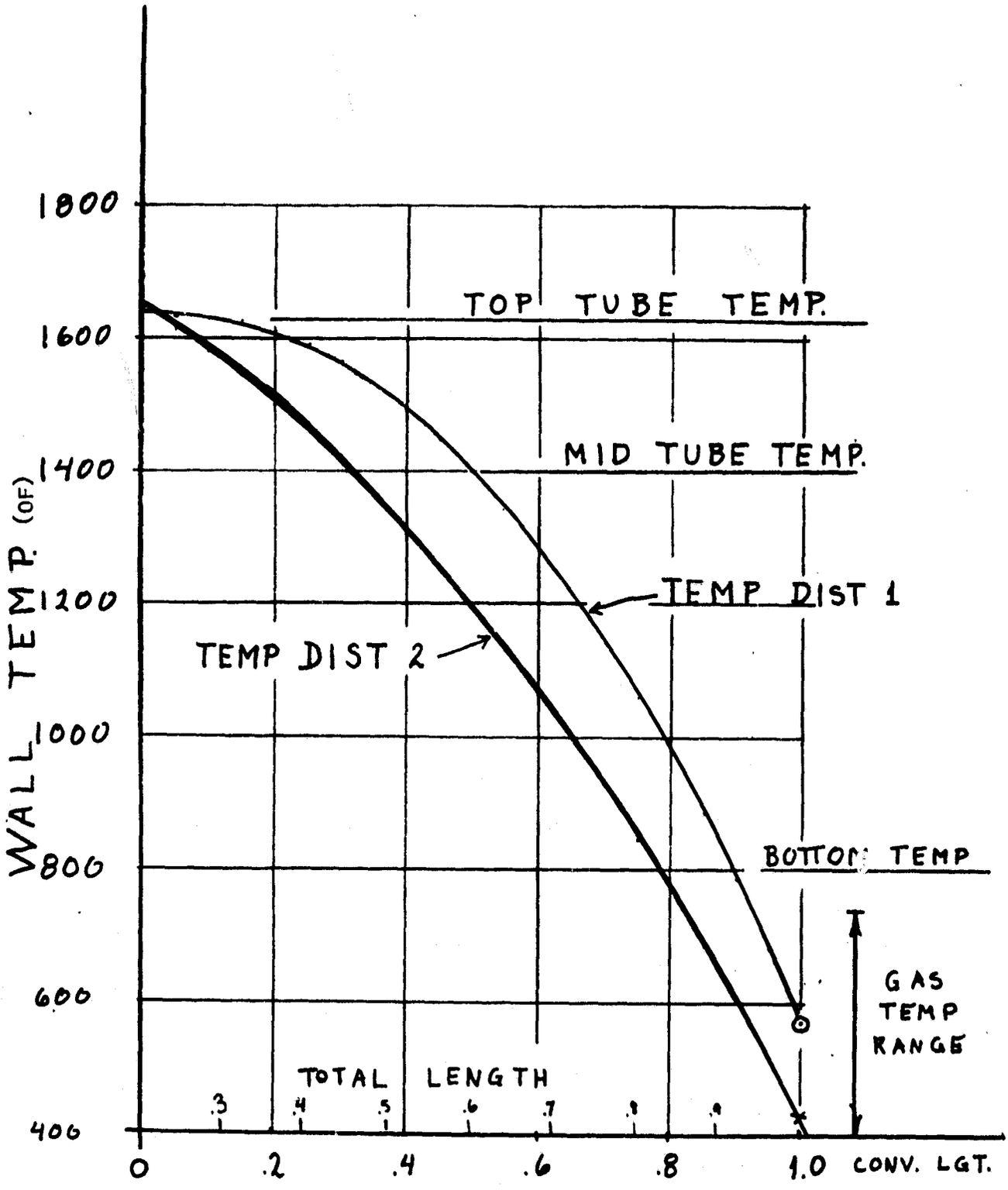
1800
1600
1400
1200
1000
800
600
400
WALL TEMP. (OF)
TOP TUBE TEMP.
MID TUBE TEMP.
TEMP DIST 1
TEMP DIST 2
BOTTOM TEMP
GAS TEMP RANGE
TOTAL LENGTH
.3
.4
.5
.6
.7
.8
.9
0
.2
.4
.6
.8
1.0
CONV. LGT.

FIGURE 14

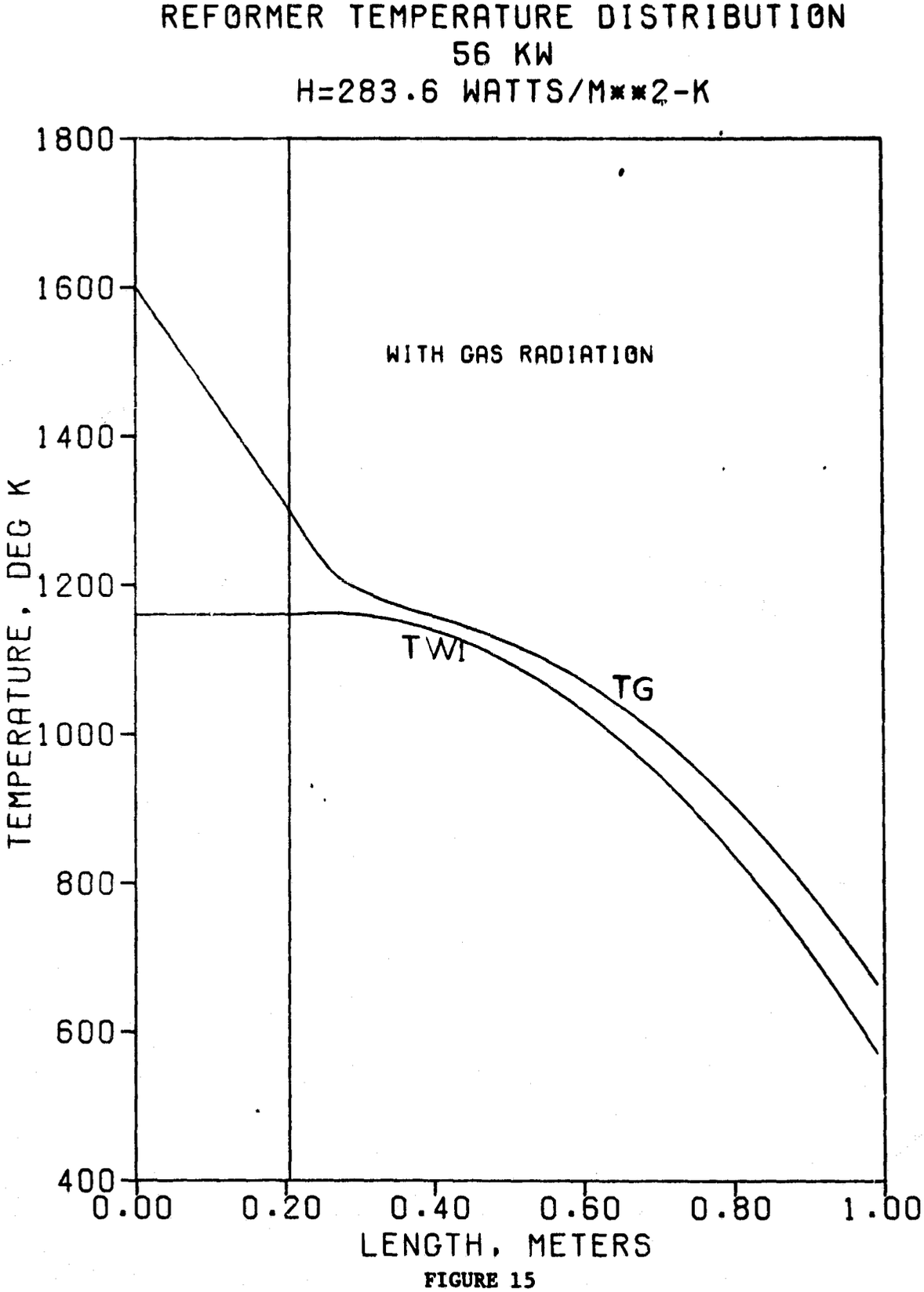
REFORMER TEMPERATURE DISTRIBUTION
56 KW
H=283.6 WATTS/M**2-K
WITH GAS RADIATION
TWI
TG
TEMPERATURE, DEG K
1800
1600
1400
1200
1000
800
600
400
0.00
0.20
0.40
0.60
0.80
1.00
LENGTH, METERS

FIGURE 15

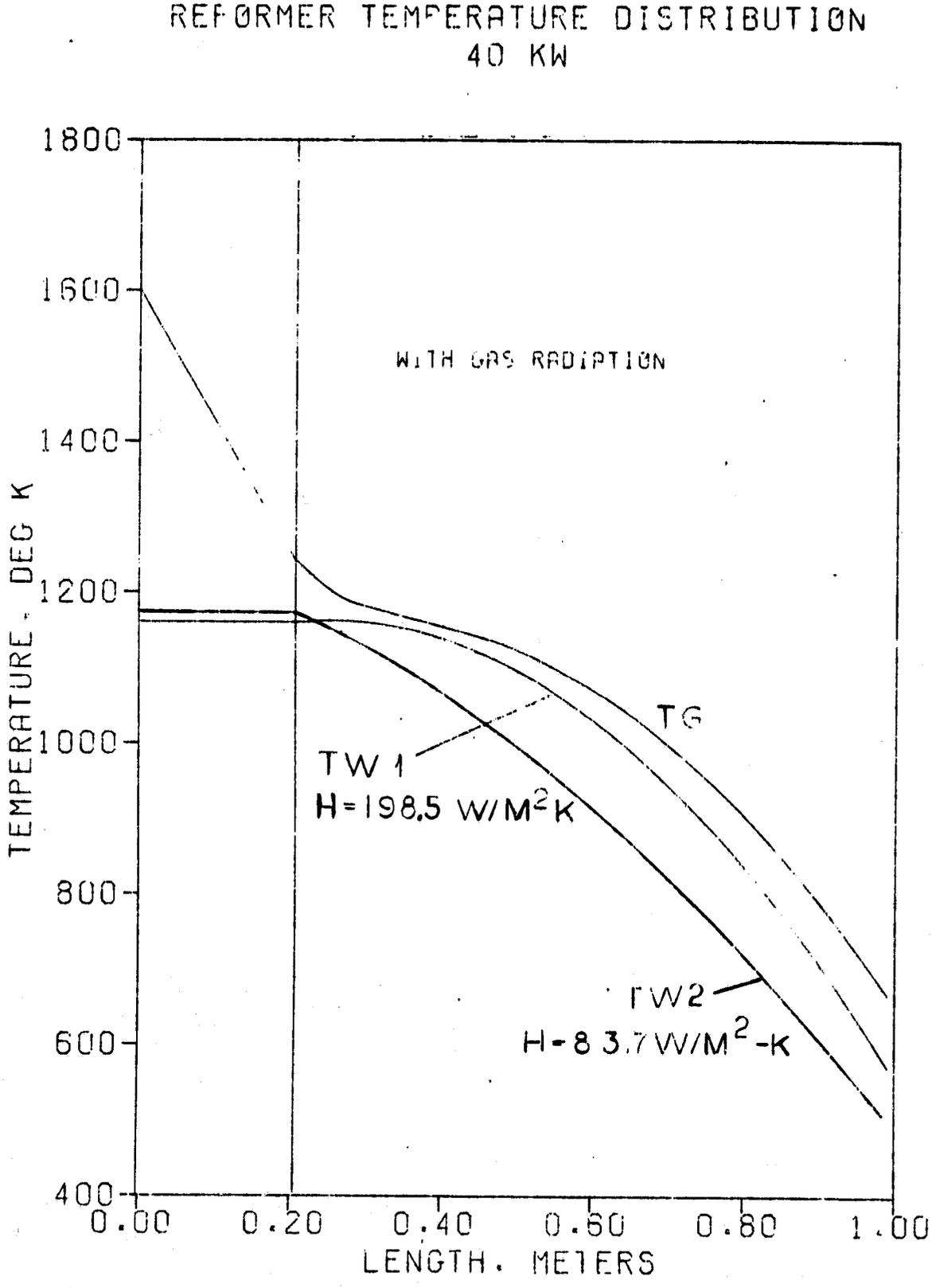
REFORMER TEMPERATURE DISTRIBUTION
40 KW
WITH GAS RADIATION
TG
TW 1
H=198.5 W/M²K
TW2
H=83.7 W/M²-K
TEMPERATURE. DEG K
LENGTH. METERS
1800
1600
1400
1200
1000
800
600
400
0.00
0.20
0.40
0.60
0.80
1.00

FIGURE 16

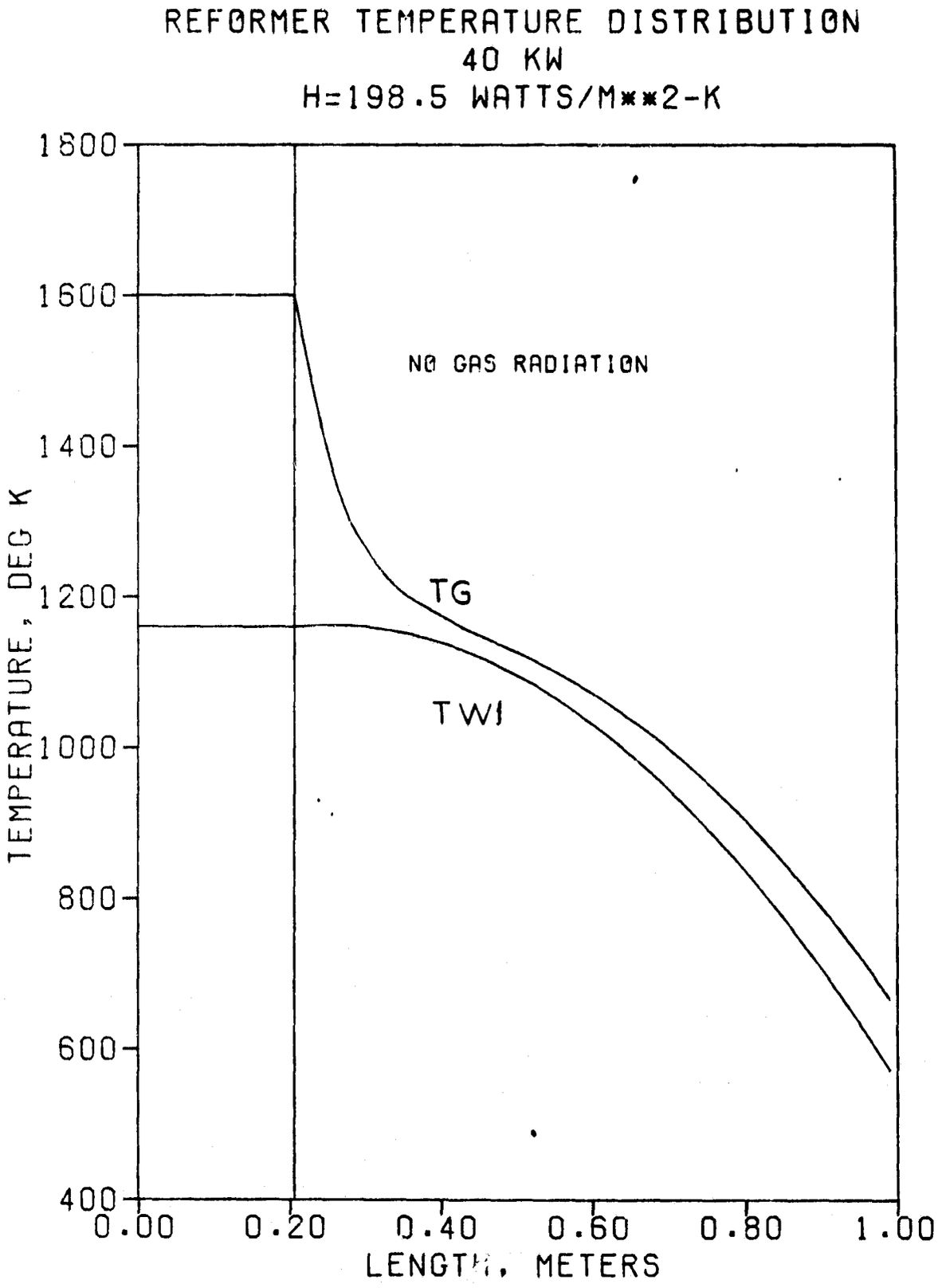
REFORMER TEMPERATURE DISTRIBUTION
40 KW
H=198.5 WATTS/M**2-K
NO GAS RADIATION
TG
TWI
TEMPERATURE, DEG K
1800
1600
1400
1200
1000
800
600
400
0.00
0.20
0.40
0.60
0.80
1.00
LENGTH, METERS

FIGURE 17

the case shown in Figure 15, the heat requirement for a 56 kilowatt case was used. A heat transfer coefficient of 50 Btu per hour feet squared °F (283.6 watts per m^2K) was required to accomplish the needed heat transfer. This case also assumes that the steam and CO_2 in the products of combustion radiate strongly to the bare reformer tube upstream of the convective section. The next curve (Figure 16) shows the 40 kilowatt case (which is a nominal operating condition) and to meet the heat load of the reformer, the heat transfer coefficient must be 35 Btu/hr $ft.^2$ °F (198.5 W/M^2 - °K). Again, this is for temperature distribution 1 which effectively provides the temperature data over the convection section only. It is also interesting to note that for the cases of no gas radiation (Figure 16) and gas radiation (Figure 17), there is virtually no difference in the convection section heat transfer coefficient to obtain the required heat transfer for the same wall temperature distribution TW1. However, if the second temperature (TW2) distribution is used, reduction in the heat transfer coefficient to 14.8 Btu/hr. $ft.^2$ - °F (83.7 W/M^2 - °K) is possible. This is due to the fact that the wall temperature is lower over the entire range than with TW1.

The heat transfer coefficients were calculated for the flows, temperatures and pressure levels of 40 kilowatt case using correlations from various sources and are shown in Table XII. This value is still higher than any value calculated. The range of calculated values is from 1.4 - 10.3 Btu/$ft.^2$ °F (8 - 59 W/M^2 - °K) with a mean of 5.75 (33 W/M^2 -°K) which are much lower than the required values.

This analysis leads to the conclusion that the data available are insufficient to provide verification of our heat transfer models.

TABLE XII

SOURCE	H (Btu/ft^2 Hr-F)	TYPE	H (W/m^2-K)
Felix & Neill[2]	5.985	Mean	33.97
Hougen & Piret[2]	10.3	Mean	58.46
Vershoor & Schuit[2]	1.96	Mean	11.13
Leva[2]	1.41	Mean	8.00
Beek[3]	4.21	Local	33.89

RMS Value of H = 5.753 (32.6 W/m^2 - °K)

Arith. Mean Value of H = 4.773 (27.1 W/m^2 - °K)

(2) W. H. McAdams "Heat Transfer", p. 290-293, McGraw-Hill Book Co., 1954

(3) Advances in Chemical Engineering, Vol. 3, p. 234, 1962, Academic Press

4.4.2 Water Conditioner Development

The UTC preliminary model specification for the on-site 40 kw fuel cell power plant[4] shows that the water treatment ion exchange bed is portable and is removed every 2000 hours and returned to the supplier for regeneration. It also shows an "acid trap", which is replaced every 8000 hours. Information in various UTC Fuel Cell Material Specifications for heat exchangers and condensers indicates an H_3PO_4 level in the process exhaust gas of about 6 parts per billion and an average gas flow of 390 pounds per hour. The resulting flow rate of H_3PO_4 is too low to be the constituent which depletes the UTC water treatment ion exchanger since the specified ion exchange bed has a removal capacity of 18,000 grains anions and 18,000 grains cations Information was requested from the NASA Program Manager on the purpose and functional capability of the "acid trap".

Several alternatives which utilize replaceable ion exchange columns were studied to eliminate equipment, rinse water, air, etc. needed for in-place bed regeneration. It was assumed that the limiting constituent would be the PO_4^{-3} from the phosphoric acid condensed with the water from the fuel cell exhaust. Commercially available ion exchange columns were used as the models in the proposed schemes. Because of the low water flow rate being used (18.1 GPH), it appears that designs with sizes for once thru ion exchange columns using conventional flows are not possible. For example, at a typical 5 GPM/ft^2 flow with 2 cu. ft. of resin, the column would be 3.3 in. in diameter and 33 ft. long. To achieve more reasonable dimensions, a water recirculating system should be used as indicated below.

At a PO_4^{-3} concentration of 106.6 ppm (6.2 grains/gal) as $CaCO_3$, the following ion exchange columns and recirculation rates can be used:

(4) FCS-0937, On-Site 40-kilowatt Fuel Cell Power Plant Preliminary Model Specification, United Technology Power Systems Division, July 12, 1978.

1 - Mixed bed IX (ion exchange), 48,000 grains capacity, 21" D x 62" H (overall) changed ∿17 days, recirculating flow of 15 gpm

1 - Mixed bed IX, 14,500 grains, 13" D x 54" H (overall), changed ∿5 days, recirculating flow of 3 gpm

3 - Mixed bed IXs in parallel, 44,300 grains total, 12" D x 56" H (each, overall), changed ∿16 days, recirculating flow 6 gpm (min.)

Using a number of smaller columns in parallel may be more desirable than a single large column because of easier handling. For each of the schemes, stand-by beds should be provided, piped into the system, to permit continuous operation. A storage tank to provide for transients and off design conditions and a pump adequate for recirculation are also required.

A survey was made of the available literature to establish if steel was suitable for service with the phosphoric acid concentrations expected in the water recovery equipment. The literature did not specifically address corrosion by H_3PO_4 at these low concentrations but the corrosion rate of carbon steel generally increased with increasing concentrations and temperatures. Pure H_3PO_4 rapidly attacked carbon steel. Conditions generally effecting corrosion include, boiling of solutions, flow velocity, dry-out surfaces, surfaces immersed partly in boiling liquid and partly in vapor, agitation aeration, stagnant areas (pockets and dead spots), suspended materials, crevices, dissimilar metals, trace impurities such as F^- and Cl^-, and time of exposure. Austenitic 316 S/S possesses good resistance to and is widely used for equipment handling H_3PO_4. Even better resistance is obtained with 316 S/S containing low carbon. Above 225°F materials such as

Hastelloys, Haynes 25, Inconel 600, 625, 825 and Carpenter 20 offer good resistance.

Prior to the specified treatment, the recovered water will have levels of H_3PO_4 which are probably no more corrosive than the water. However, testing of the actual material being used, under operating conditions, is suggested as a means of avoiding any unanticipated results.

4.4.3 Other Ancillary Systems Development

A control system was identified as one ancillary system requiring substantial attention. It was decided that a complete control system package be specified - one capable of monitoring and controlling each individual component in the OS/IES proof-of-concept plant. Operation of such a system will answer critical questions regarding the operating cycle and ultimately would show which controls are essential in the commercial plants.

A typical diagram of a fuel conditioner sybsystem is shown in Figure 18. The major components (in addition to the fuel cell modules) are three heat exchangers, a desulfurizer, a shift converter, a steam generator and superheater, a reformer, and a standby processed gas supply. Ancillary components, valves, pressure gauges, and measuring instrumentation are shown in a more detailed diagram (Figure 19).

The function of the OS/IES fuel cell modules is to supply the electrical load as required. To do this in an efficient and flexible manner, the fuel cell subsystem has four 30 kW modules. To provide fast response and maximum flexibility, batteries have been shown in the system. Switching the output of the individual stacks will provide a means of charging any battery with any stack or combination thereof so that, in case of a stack failure, full load voltage can be maintained.

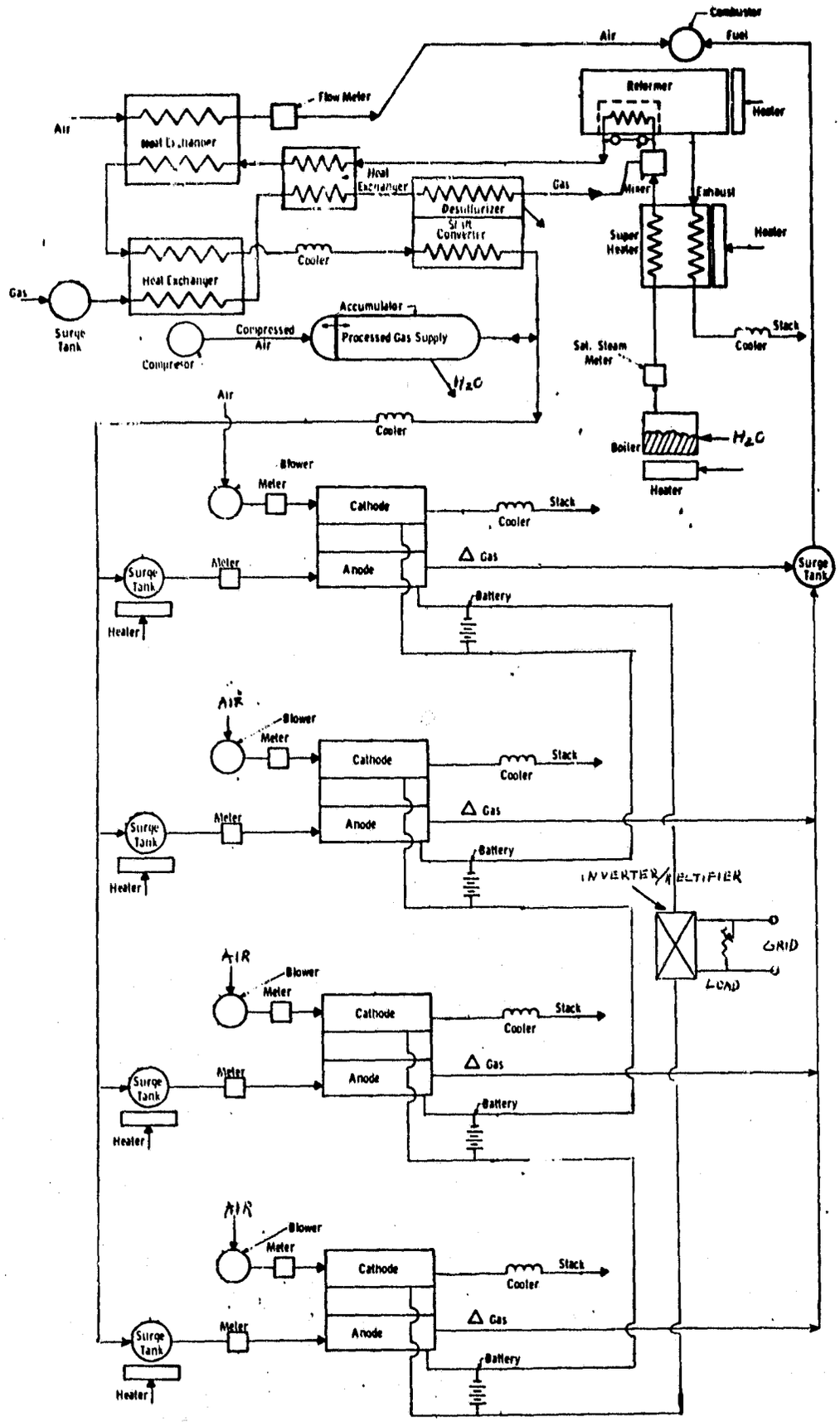

FIGURE 18 OS/IES MAJOR COMPONENTS

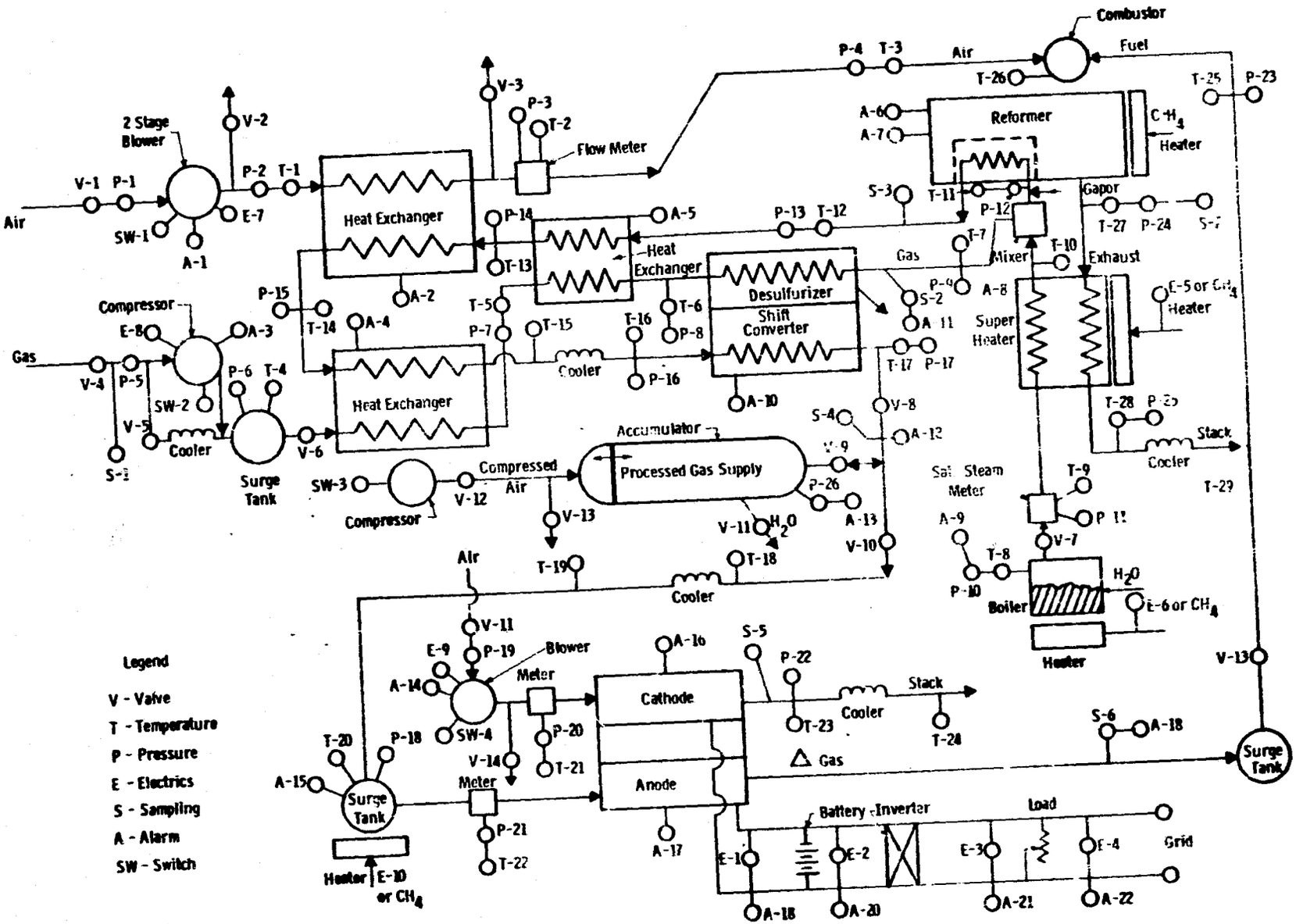

FIGURE 19 OS/IES CONTROLS AND INSTRUMENTATION

If the system is tied into the grid, any overload (beyond the 120 kW capacity of the fuel cell) could be supplied by the grid or, for short times, by the battery. The inverter also may serve as a rectifier so that the batteries could be charged from the grid.

In addition to overload and failure protection, batteries can provide instant load following which the fuel conditioner/fuel cell combination is not able to do, and can be used for starting the plant in the absence of the grid (black start).

In the second quarterly report of Phase I, the matter of utility standby power was addressed. The cost for 110 kW as "dedicated standby" was shown as $860 per month and "if available standby" as $110 per month. If we supplement or replace this with a battery bank the following possibilities arise:

(a) Assume six standard 12 volt lead acid batteries in series for each module. If two banks are connected in series, total open circuit voltage at the inverter will be 144 volts. For a 120 kW load at 120 volts the current per bank of 24 batteries will be 500 amps which could be tolerated for a minute or less - long enough to bring the fuel cell into operation. During off peak times, requiring perhaps 10% load, the battery storage could produce 50 amps for an hour.

The cost of 24 batteries at $50 each would be $1200 and if their lives were assumed to be three years, this would be equivalent to $400 a year or $33 a month. Recall that the dedicated standby for 110 kW was $860 per month. Perhaps some combination could be worked out with, for example, 30 kW standby at $250 per month and the balance from the storage battery. This could represent greater reliability at somewhat increased cost.

(b) Assume 10 times as many storage batteries, i.e., 240. The cost becomes $333 a month - still less than the cost of "dedicated standby". It would now be possible to run off the batteries for nearly one hour at normal loads, or to run for 10 hours at 10% load - perhaps all night, thereby permitting the fuel cell to be shut down. It is also possible to run on two of the four stacks or to take power off the grid at night - possibly at reduced rates. One disadvantage of so many storage batteries would be the space required - probably about 4 ft. x 8 ft. and 5 ft. high plus room for maintenance access.

Returning now to Figure 18, and tracing the fuel system, we see gas proceeding through a desulfurizer, mixing with steam and entering the reformer. Leaving the reformer it is cooled in three heat exchangers, simultaneously heating the raw fuel and air. The cooled gas enters the shift converter where the conversion process is completed and the fuel is ready for the fuel cell. The steam generator is shown in two parts, a boiler, always at pressure and on hot standby, and a superheater receiving heat from the reformer, supplemented by additional firing as needed. Air is shown entering the cathode and also supplied to a combustor which with partially depleted fuel from the anode heats the reformer and subsequently the steam superheater. Several surge chambers will be seen throughout the system to smooth load follow capabilities.

The fuel cell is reported to have a fast response time, reaching load in perhaps a second. (However, this may not be fast enough, therefore, the battery storage or grid tiein). But wherever heat exchangers and catalytic reactors are involved, response time could be 10 or 15 seconds to full load. Therefore, a supply of processed gas which is capable of feeding directly into the fuel cell modules is shown. It will be filled during off peak operation and pressurized in

an accumulator either hydraulically or with compressed air. Now when a rapid increase in power is called for, or during startup, use can be made of this supply without waiting for the heat exchangers to begin functioning.

Figure 19 shows a schematic diagram of the OS/IES with the proposed location of the various valves and instruments. Only one of the four fuel cell stacks is shown, and as in the case of Figure 18, only those components directly associated with fuel processing. Nothing has been shown for the water treatment system or for special start-up or shut down hardware although this will all be tied into the master controller. With reference to the legend, these are indicated:

29 valves	16 Voltage pickups
7 switches	16 current indicators
50 thermocouples	13 sampling probes
40 transducers	40 warning alarms

It should be pointed out that these measurements in general have to do with the process. For a prototype system, more monitoring of the stacks is recommended with temperatures and strains measured at many points. This would also apply to other components.

With reference to these schematic diagrams, a preliminary specification for a microprocessor was written (Appendix B). Copies have also been give to other Westinghouse Divisions, where there are similar microprocessors or where they have worked with them, for comment.

The specific requirements for the microprocessor are:

To start and stop the OS/IES.

To record and display a variety of pressures, temperatures voltages, and currents.

To compute flows, gas compositions, and electric power.
To control the operation of each component in harmony with all other components.
To monitor the functions of each component.
To indicate an off design uncontrollable condition.
To shut down a portion or all of the OS/IES in the event of a dangerous or potentially damaging condition.

The microprocessor to be specified will be capable of monitoring all the points shown in the diagram with appropriate spares and controlling the operation of each component individually. Eventually most of the control points and sampling probes may be found unnecessary. However, until we learn to operate the complete unit and determine the time responses of the components, it will be necessary to monitor all the points indicated. Extra channels will be provided to accommodate readings that we may have overlooked.

The prototype version of the microprocessor should be portable and capable of being moved to a site where a specific component is being fabricated and tested. Learning to operate these components singly is necessary before trying to control the whole OS/IES assembly. Eventually the required control and monitoring points will be identified and these together with established component response times will lead to a second specification for a microprocessor to be included as part of the OS/IES package.

With comments obtained from those who have reviewed the preliminary specification, a revised specification will be prepared and submitted to Westinghouse Management Systems and Services (MS&S) as required by Management Directive MD-D10 dated August 1979. With the approval of MS&S, copies of the preliminary specification will be supplied to R&D Purchasing for release to obtain costs from potential microprocessor suppliers.

4.8 Computer Model

The REPENT program for the tubular methane reformer kinetic model was completed in January. A report has been typed and the figures completed by the drafting department. It is in the review process, and should be formally issued by the end of April. This report details the model's derivation from the first principles, pertinent specifics of the computer programming, and gives preliminary parametric studies and results.

The BOLTAR program, which is a more flexible version of REPENT, is now completely debugged and working on both flat slab and tubular geometries with either co-current or counter-current flow arrangements.

A report on the BOLTAR program has also been written. This report outlines the different models in BOLTAR, program access and use and results. This report, completed in March, will be issued for review once it is adjusted to function with the higher catalyst activity that ERC is presently finding in their experimental work.

The BOLTAR program allows the user to exercise considerable flexibility. Options include:

(a) inclusion/deletion of the water gas shift reaction
(b) flat slab or tubular geometry
(c) co-current or counter-current flow arrangement
(d) different outside heat transfer correlations
(e) arbitrary heat transfer factor

All of the different models in the program have been exercised and are working properly. Input data includes reformer gas inlet temperature and component flow rates, combustion gas inlet temperature and component

flow rates (or the metal wall temperature profile), the reformer gas pressure (assumed constant), catalytic parameters, and the dimensions for the appropriate geometry. Output includes the reformer gas conversion profiles, equilibrium constants, reformer temperature profiles, heat transfer information, and reformer gas exit flow rates and composition.

Program results are:

1. The flat slab geometry has slight (∿5%) conversion advantages over tubular designs for equivalent conditions. This is due to the larger heat transfer area per unit bed volume.

2. The external (combustion gas) heat transfer resistance is the dominant one for the tubular geometries tested. However, the internal resistance is the dominant one for the flat slab geometries tested, producing higher metal wall temperatures. Efforts have been made to increase the combustion gas flow rate and lower its temperature (same relative heat capacity), and, hence, produce similar reformer results with a lower metal wall temperature (<1900F). This involves doubling the combustion to reformer gas ratio used by UTC (to 3:1 from 1.5:1).

3. The co-current flow arrangement is equilibrium limited, and, therefore, little gain can be made using higher activity catalysts.

4. Counter-current flow is more thermally efficient than co-current flow.

5. Counter-current flow can attain higher conversions (∿10%) than co-current flow at the lower space velocities, and this advantage increases with higher activity catalysts.

6. Preliminary ERC catalyst data indicate an Arrhenius frequency factor of 1×10^6 [(lb mol/hr.)/(lb cat./atm CH_4)]. Insertion of this value into the program causes it to fail. The program has been run with frequency factors as high as 2×10^5.

7. The program has reproduced Phillips Petroleum reformer data to within 5.5% on conversion and 40°F on exit temperature. It can approximate UTC information in a tube 25% longer, but gives a 100°F higher exit temperature.

TASK 5: MANAGEMENT REPORTING AND DOCUMENTATION

5.1 Supervision and Coordination

Technical Review Meetings

A review meeting of members of the NASA technical management team, Westinghouse, and ERC personnel was held. The major topics discussed were the on-going fuel conditioning work (with emphasis on the fuel definition), the design of the ERC 8 kW test loop and plans for stack fabrication.

Coordinating Meetings

Several meetings were held to coordinate the Westinghouse and ERC effort to provide the fuel cell component and stack assembly procedures and test stand documentation required by the NASA Project Manager. The resultant documents were delivered to and approved by the NASA Project Manager.

Planning Meeting

A meeting among NASA, (W) and ERC team members was held to discuss the status of the MK-1 and MK-2 cell technology and ways to advance it. As a result of the interactive discussions, an innovative method of acid replenishment was devised and plans for proceeding with stack fabrication were made.

ERC Subcontract

NASA approval of the ERC subcontract, subject to minor modifications, was received. These modifications were transmitted to and accepted by ERC. The formal signing should occur early in the next quarter.

Advisory Committee Meeting

The first meeting of the Advisory Committee, described in the proposal for this contract, was held at the (W) R&D Center on March 18. To provide perspective, the prepared talks summarized the Phase I effort, ERC work on their technology contract, in-house (W) work on PAFC, and the plans for the electric utility commercial prototype as well as the work on this project. The Advisory Committee Chairman concluded the meeting by promising to prepare a report summarizing the salient points of the wide ranging discussions.

Work Approvals

Based on approvals recived from the NASA Project Manager, ERC was advised to begin procurement for and construction of a test stand for short stacks of the MK-1 configuration and to proceed with fabrication of cell components and cooling plate blanks for a MK-1 short stack and cell components for a MK-2 simulated stack.

5.2 Documentation and Reporting

Status and Management Reports

The First Quarterly Report was submitted to and approved by the NASA Project Manager and will be distributed to the specified recipients early in the third quarter.

The technical status reports for January and February were submitted for approval. Approval of the January report was received and it will be distributed early in the third quarter.

The required management reports (533M and 533P) for December, January and February were prepared and submitted.

The management plan for the Third Quarter (533Q) was prepared and submitted.

Fabrication Procedures and Designs

A description of the procedures to be followed in fabricating cell components was submitted to and approved by the NASA Project Manager.

A description of the 2 and 8 kW test facilities, including revised cost estimates, to be built at ERC were submitted to and approved by the NASA Project Manager.

A description of the procedures to be followed in assembling a MK-1 short stack and a MK-2 simulated stack were submitted to the NASA Project Manager for review and/or approval. These procedures incorporate the innovative scheme for acid addition devised in a meeting at NASA-LeRC.

5.3 Planning

No work scheduled.

III. PROBLEMS

Fuel cell stack design and fabrication are behind schedule. As reported earlier, this is partly due to a halt in work pending successful demonstration of the 30 x 43 cm cell technology and partly to a delay in providing an adequate list of cell fabrication and stack assembly procedures to the NASA Project Manager. These have now been resolved. However, the delays have disrupted the ERC production schedules and future progress may be somewhat slower than originally planned.

Stack 557 (5-cell-MK-2) took about three times as long to wick as standard 5 cell stacks with straight-through channels. This may be caused by the design itself, i.e., the MK-2 design pattern may exert pressure against the wicking direction from both sides of the matrices. The stack will be rebuilt using wet assembly and an innovative acid addition scheme to eliminate this problem.

IV. PLANS

Task 1: Design of Large Cell Stacks

Patent disclosures describing enclosure design features and stack assembly procedures will be written and submitted to the NASA Contracting Officer and Project Manager. A plan to evaluate the enclosure design features and assembly procedures in the MK-3 modules will be developed. Results of the thermal management analysis and tests will be incorporated in the enclosure design work.

A review of the full scale module enclosure design and assembly procedures with the NASA Program Manager is scheduled for April 8.

The design and assembly procedures for a MK-1 short stack will be submitted to the NASA Project Manager for approval.

Work on cooling plate assembly, thermal management of stack hardware, tie bar configuration, compression loading, electrolyte filling, and manifolding will continue.

Task 2: Stack Fabrication

Fabrication of a new Mark II simulated (5-cell) stack (No. 558) is scheduled to be completed by the end of April and testing at ERC is anticipated to be completed in mid May. The bipolar plates from Stack 557 were salvaged after post-test and will be reused for Stack 558. The fabrication of other electrochemical components is scheduled.

Fabrication of components for the second Mark I, 23-cell, short stack has been initiated and scheduled for completion by the end of May. Pretesting at ERC is scheduled in early July after which the stack will be transferred to (W) R&D for further testing.

Corroborating experiments will continue in the areas of cooling plate assembly, electrolyte filling, and stack compression.

To verify the theoretical predictions of stack thermal behavior, a series of corroborating experiments is in progress. A 13 cm x 38 cm 80-cell stack containing Mat-1 matrices is under observation. The changes in the stack dimensions and compression will be measured. Experiments have also been initiated to investigate the thermal behavior of wet matrices, shims and electrode materials. The above information will be used in designing the hardware for the subscale stacks.

The latest costs of machining bipolar and bipolar/cooling plates have been lower than anticipated. An analysis of the costs and scheduling requirements of molding vs. machining will be performed to determine the most effective way of producing these components for future test stacks.

Compression tests using ribbed structures of the Mark I and Mark II designs will be performed on the matrices, electrodes, and backing paper. An attempt will be made to determine the degree of deformation in the compressed components in the groove area between the ribs.

Task 3: Stack Tests

Testing of the second 5-cell MK-2 stack (No. 558) will be initiated as soon as fabrication is complete. This is currently scheduled for the end of April. The test objectives and plan will be the same as those developed for Stack No. 557.

Pretesting of the second 23-cell stack of the MK-1 design is scheduled to begin in July. A test plan, including objective standards

for acceptable performance, will be submitted to the NASA Program Manager for approval at least three weeks prior to the start of pretesting.

Task 4: Fuel Conditioner Development

4.1 Fuel and Water Definition

The definition of fuels to be considered for this program is essentially complete. A minimal effort will be continued to keep abreast of any changes in the situation and/or evaluate new information which becomes available.

The water definition for the case where water is recovered from the system will be adjusted as new information becomes available.

4.3 Technical Data Base

The test program for Haldor Topsoe's RKNR catalyst is presently in Part 1 of Step I of the plan described below:

Step 1

Since the catalyst activity is unknown, the first experiment will be used to determine the appropriate catalyst weight and space velocity to be used so that the conversion remains less than 20%.

This experiment will therefore proceed as follows:

1. Catalyst weight 0.5 crushed 16-20 mesh catalyst
   temperature 550°C
   Gas Composition .2H_2, .10CH_4, .20H_2O, .68He
   The total flow will be adjusted to obtain 5% - 20% conversion

2. Gas composition will be changed to: $.02H_2$, $.30CH_4$, $.60H_2O$, .08He

   Again the total flow will be adjusted to obtain 5% - 20% conversion

It will proceed to Step II work in April. Step II will include the range of conditions and gas compositions as follows:

Step II

After choosing an appropriate space velocity and catalyst weight based on the experiment in Step I, the following matrix of experiments will be performed.

	Temp.	Gas Composition			
1.	450°C	$.02H_2$	$.10CH_4$	$.20H_2O$	.68He
	550°C	"	"	"	"
	650°C	"	"	"	"
2.	450°C	$.02H_2$	$.10CH_4$	$.40H_2O$	.48He
	550°C	"	"	"	"
	650°C	"	"	"	"
3.	450°C	$.02H_2$	$.20CH_4$	$.40H_2O$	.38He
	550°C	"	"	"	"
	650°C	"	"	"	"
4.	450°C	$.02H_2$	$.20CH_4$	$.60H_2O$	.18He
	550°C	"	"	"	"
	650°C	"	"	"	"
5.	450°C	$.02H_2$	$.30CH_4$	$.60H_2O$	.08He
	550°C	"	"	"	"
	650°C	"	"	"	"

Step III

Repeat Step I with catalyst pellets

Step IV

Repeat Step II with catalyst pellets

Approximate time for each catalyst is five weeks

Problem areas in catalyst utilization, involving carbon deposition from olefins, olefin producing compounds, and aromatics, and involving sulfur poisoning from mercaptans, thiophenes, and H_2S will also be investigated. Data from Step I testing will be reported in the April Progress Report.

4.4 Ancillary Equipment Data Base

All major equipment for the burner test facility has been received. Design of the burner and heat exchanger components is nearly complete and fabrication should start in April. Assembly of the test stand will start in April and should be completed by the end of the next quarter.

Evaluation of the control requirements for the fuel conditioner subsystem will be continued and the schematic diagram and microprocessor specification will be modified as required

4.8 Computer Model

The BOLTAR program is essentially completed. Future work will include adjusting the program to accept higher frequency factors, and program modification as necessary to reproduce experimental data as it becomes available. Parametric studies will continue to be performed as necessary.

Task 5: Management and Documentation

5.1 Supervision and Coordination

Coordination of efforts among the task leaders and between ERC and Westinghouse will be continued.

A review and planning meeting for the NASA Program Manager and his team is scheduled for April 8 and 9.

A meeting of the Program Advisory Committee (composed of Westinghouse and ERC management personnel) will be scheduled for the fourth quarter.

Presentation to and meetings with DOE personnel will be scheduled as requested.

5.2 Reporting and Documentation

The task leaders' inputs to the Technical Status Reports will be edited and the reports will be submitted to the NASA Technical Manager for patent approval. The management reports will also be prepared and submitted to the NASA Technical Manager.

5.3 Planning

No work is scheduled for the third quarter.

APPENDIX A

EXPERIMENTAL VERIFICATION OF ACID ADDITION VIA SCHEME I

An experiment was performed, with two bipolar plates and materials, to verify the ability of Scheme I to feed acid to each cell matrix. In this experiment, acid was dripped into the acid fill hole and as the first (top) matrix became saturated with acid, it began to drip acid to the cell matrix below. Increasing or decreasing the rate of acid addition to the acid fill hole resulted in a corresponding change in the drip rate to the cell matrix below it. At no time, was there a build-up of acid above the matrix greater than 1/8 in. As acid was added to each cell matrix, it would wet and fill the pores in the matrix away from the hole. The total time required to fill the pores of the entire matrix was not established in this experiment. This scheme (I) is to be incorporated in the plans for the new Mark II stack build.

APPENDIX B

EQUIPMENT SPECIFICATION - PRELIMINARY March 27, 1980

FUEL CELL MICROPROCESSOR FACILITY

1. SCOPE

This preliminary specification covers the requirements of a microprocessor to function with a fuel processing/fuel cell subsystem. In brief it must preprogram, monitor, control, and log data for the complete subsystem. Heat recovery portions of the system for water and space heating will be added later, and are estimated to double the heat exchange complexity shown.

2. DEFINITION OF SYSTEM

The system comprises five major components:

- Desulfurizing
- Reformer
- Shift Converter
- Steam Generator
- Fuel Cell

The first four of these components prepare the fuel for use in the fuel cell. In addition to the major components there are several ancillary components consisting of at least four heat exchangers and five heat recovery coolers, a gas compressor and blower, gas storage bottles, meters, burners, heaters, valves and many monitoring points. The electrical system includes a rectifier, an inverter, storage, and more monitoring and controlling instrumentation as well as complex switching. The heat recovery usage for the system is not shown on the diagram for this system.

3. SYSTEM OPERATION

The various monitoring and control points may be seen with reference to the flow diagram of Figure 19. Following through the diagram, fuel (natural gas) is compressed, heated, and passed through a desulfurizer. It is mixed with steam, entering a reformer. From the reformer it passes through exchangers and a shift converter and then to the fuel cell. Because of the nature of the process at various steps, it is necessary to cool or heat the fuel, hence the heat exchangers and coolers. Air is added by a blower at two points in the cycle. Cathode gas is recirculated with appropriate makeup and venting and the anode product is returned and burned in the reformer and from there it is used to superheat steam. Because of reaction time delays in some of the components, storage supplies and surge vessels are used. Storage in the form of electrical energy i.e., battery is also shown. This is essential if a grid supply is unavailable and it may operate in conjunction with the grid either for start up or faster load following. Four fuel cell assemblies with individual monitoring and controls are anticipated.

3. FACILITY OPERATION

The Microprocessor Facility will be required to preprogram, monitor, and control the complete system. To this end it must start and stop the unit and make appropriate changes in the operation of each component to follow the electrical load cycle.

The primary input to the facility will be an indication of electrical load demand. On the basis of this signal, the microprocessor will provide signals to the appropriate controllers to supply process gas to the fuel cells and/or storage.

A secondary input will be indications of trouble (malfunction, over temperature, dangerous gas composition, etc.) which may activate an alarm or shut down the system if the alarm is ignored or the problem uncorrectable, or if the malfunction is instantaneously dangerous. This control must be overriding on the process control.

At this time the following items have been identified with the associated function (with reference to Figure 19):

Item	Number	Function
(A) Alarm Indicators	40	Monitor and Control - Input
(P) Pressure Indicators	44	Monitor
(T) Temperature Indicators	50	Monitor
(S) Gas Samplers	13	Monitor
(E) Electrical Instruments	16	Monitor and Control - Input
(V) Valves and Switches	40	Control - Output

Some of these serve a duplicate function as will be noted, for example, alarm monitor and control.

All inputs will be in the form of electrical signals, from thermocouples, pressure transducers, gas analyzers, and battery specific gravity. All outputs will also be electrical although they may control either electrically operated or pneumatic valves.

4. FACILITY REQUIREMENT

A microprocessor facility is required which will monitor and record 150 pressures, temperatures, currents, voltages, and gas compositions.

The facility must control the process from startup through a load following function to shutdown, through the operation of 40 valves and switches.

The facility must also monitor 40 alarm stations, signalling trouble and/or shutting down the system. This function must be overriding.

Load following and the alarm systems must be followed continuously. Speed and frequency of recording data are not critical. The recorded data should be visual as well as on paper and/or magnetic tape compatible with the existing computers.

The facility should be portable -- for use at various sites. It is intended at this point for use on prototype test stands and for evaluation and process development. Eventually its use will be narrowed down to a specification for a microprocessor for the OS/IES installation.